Chemical Mechanical Polishing of InSb

Master's Thesis for Degree in Nanoscience

Written by David Michael Linehan

Department of Electrical and Information Technology

Lund University

Supervised by Mattias Borg

Examined by Erik Lind

LUND UNIVERSITY

2021

Abstract

This project studies, with the aid of Atomic Force Microscopy (AFM), profilometry and optical microscopy, how InSb samples with etched holes (floored with W) polish when undergoing Chemical Mechanical Polishing (CMP). It is found that a mix of $NaOCl: DI$(1:10) + $C_6H_8O_7: DI$(1:2) as a CMP slurry is sufficient for etching, though it results in a rough texture at the global scale. A large downward pressure is found to increase global etch consistency but results in a rough nanoscale surface. A low downward pressure decreases etch speed, while cleaving the W floors from the holes and causing an inconsistent nanoscale roughness. A high rotational plate speed is found to increase the global etch rate somewhat, but provides a very consistent, smooth surface at the nanoscale. Ultrasonic baths are found to be effective at cleaning larger debris from the sample, while PVA (Polyvinyl Alcohol) sponges do the same for smaller particles. Polishing samples in one run, as opposed to polishing the same sample multiple times, appears to give better results in every regard, which may be due to effects of surface contamination.

Contents

1 Introduction 1
2 Background 2
2.1 Sample Materials 2
2.2 CMP 2
2.3 Surface Topology Measurement 4
3 Experiment 6
3.1 Setup 6
3.2 Preparation of Sample 8
3.3 Analysis of Sample 9
4 Results and Discussion 11
4.1 Etch Rate 11
4.2 Sample Cleanliness – Nanoscale 13
4.3 Sample Roughness 16
4.4 Sample Cleanliness – Global Scale 17
4.5 Final Samples 23
5 Conclusion 29
6 Outlook 30
References 32

1 Introduction

Technology is in a constant race to get smaller. Not just the thinness of a phone, or compactness of a camera, but also the components that drive these devices. The shrinking of these components is no mere vanity project, however. For example, smaller transistors use less energy and possess greater computing power than their larger counterparts. This can also lead to a decrease in the heat generated by these devices, allowing them to remain at their optimal operating temperature longer. While the use of smaller electronics components provides only benefits, the fabrication of such devices can pose problems. A number of these problems arise from the surface of each layer of the device. These surfaces can have defects or intentionally created features with some height. The height of these features is relatively greater when using thinner layers and can eventually cause problems. Two such problems come when, for example, a transistor is covered with a dielectric film. If, for example, the gate is placed such that it is taller than the substrate, the dielectric will also have some bumps above where the gate is. Depositing a layer of metal onto this dielectric will transfer this bump to the metal layer. The first problem that arises here is that while the metal on the top bottom of this bump are connected, the metal narrows considerably at the boundary, relative to the thickness in the flat regions. This leads to a decrease in the wire's cross-section, and a proportional increase in its resistivity at those points. The height difference between the bump above the gate and the substrate can also cause problems for lithography of miniscule features, as the lithography technique may not be able to focus on both levels. As layers stack upon layers, these problems compound until the device is no longer usable.

The solution to these problems is to planarize the device after critical steps. For example, the same transistor could have an excess of dielectric spread over it. The bumpy features will still exist above the gate, but now, using a tool such as CMP (chemical mechanical polishing), the raised regions can be polished away, leaving a flat layer of dielectric. Depositing metal onto this surface will also give a flat layer of that metal. A tool such as CMP also makes the so-called Damascene process possible. This process allows for filling an etched hole or trench in a dielectric with a metal and removing the metal elsewhere, in order to connect stacked layers to one another. The process complements deposition and etch-processes, avoids the space wasting of sloped vias, as well as skips around the problem of some metals not being easily etchable. A dual Damascene process can lay down inter- and intra-level wiring in the same process step [1].

With such benefits, it's no surprise that major manufacturers use CMP in their production lines. Less commonly used with CMP, however, is InSb. InSb is a III-V material with excellent infrared capabilities due to its narrow energy band gap of only 0.18 eV [2], making it uniquely sensitive to optical signals up to 7 µm wavelength. Optoelectronic devices are very sensitive to rough surfaces, which can lead to unwanted nonradiative recombination, and CMP could be a beneficial tool in fabrication of such devices but there has been little study of how to polish InSb using CMP. Therefore, throughout this work, it was examined how various parameters of CMP might influence InSb's MRR (material removal rate) both locally and globally, the surface roughness at both the microscopic and nanoscopic scales, as well as methods of cleaning InSb after polishing. To study these qualities, a variety of microscopes and surface profilers were used; namely optical microscopy, Atomic Force Microscopy (AFM), and profilometry.

2 Background

2.1 Sample Materials

Indium Antimonide - InSb

Indium Antimonide (InSb) is a so called III-V material. This means that Indium resides in group III of the periodic table and has three valence electrons, while Antimony from group V has five valence electrons. III-V materials are invaluable for their impressive electrical properties, such as their high electron mobilities, low exciton binding energies, and many having direct band gaps [2]. Optoelectronics benefit particularly from the direct band gap, as it is necessary for the efficient emission of light [2]. InSb, having the lowest band gap of all III-V materials (0.18 eV [2] at room temperature), is therefore of great utility where infrared light is of interest. InSb is quite a soft material, with a Vickers microhardness of 230 HV [3] [4]. Along with being a soft material, InSb is also rather brittle, and therefore care is needed when handling the material. In a project related to this thesis work, InSb is deposited using low-temperature molecular beam epitaxy, and when formed has a surface roughness on the scale of 3 nm [5]. For utilization of these InSb films in a recrystallization process it is vital to improve this roughness value below at least 1 nm, preferably below 0.5 nm. InSb can wet etch in a citric acid solution and be polished by CMP using citric acid and NaOCl [6].

Tungsten - W

Tungsten is an exceptionally hard metal with a Vickers microhardness of about 343 HV [7]. Tungsten is not notably etched by citric acid [8].In this project, W is used as a polishing stop layer, where the high hardness of the material compared to InSb makes it resistant to the CMP process and acts as a good marker layer.

2.2 CMP

Chemical mechanical polishing (or planarization) (CMP) is, as its name suggests, a planarization technique which uses both chemical and mechanical means to achieve a surface with ideally monolayer roughness. While a purely chemical etching technique (such as wet etching) can be performed in a beaker, and a purely mechanical form of polishing (such as sanding) can be done with a handheld abrasive, CMP requires an integrated setup in order to fine tune the interaction between the chemical and mechanical components. There are four types of commonly used, commercially available CMP set-ups that one might run into [9], but they function, in principle, in largely similar manners to each other. Therefore, just one type shall be focused on here; a rotary-type polisher along with a sample carrier which moves laterally along the polisher's radius. This type of CMP shall also be the type of CMP used throughout this study. The general physical layout of such a CMP can be seen in Figure 1. All these components work in tandem with one another to influence the material removal rate (MRR), surface quality, and uniformity.

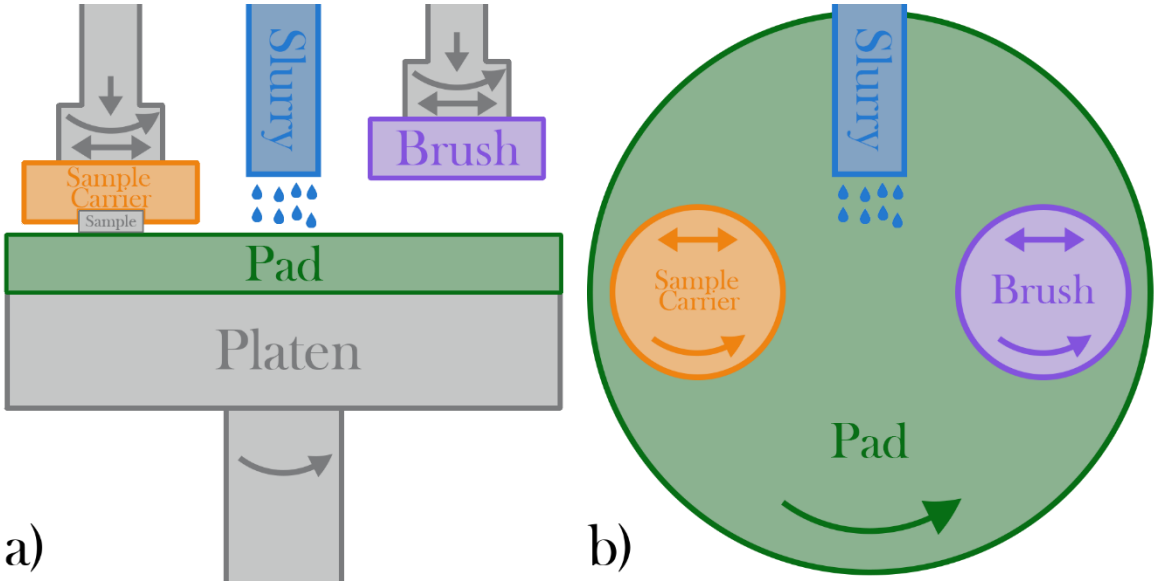

Figure 1: A rotary type CMP with a reciprocation sample carrier. a) shows a side view, while b) shows a top-down view of the same setup. The curved arrows denote that rotation is possible, the straight double headed arrow denotes that a side-to-side reciprocatory motion is possible, while the downward arrow denote that a motion downward with some resulting pressure is possible.

The chemical component of CMP comes in the form of a slurry (a mixture of solids suspended in a liquid) which is dispensed directly onto the pad, as shown in Figure 1. The liquid part of the slurry is a mix of DI water and other chemicals which, apart from the individual chemicals effect, will give the slurry either an acidic, basic, or neutral pH. The chemical components and pH both play a role in the overall polishing quality [10]. The solids in the slurry contribute to the mechanical portion of CMP. The solid part of the slurry comes in the form of abrasive particles (such as Al_2O_3, CeO_2, SiO_2) ranging from 10 to 100 nm [9]. This solid portion is critical when polishing harder materials, but when dealing with softer materials (such as certain III-V semiconductors) it is sufficient (and perhaps ideal) to forgo the inclusion of abrasives. Previously, a combination of $NaOCl$ (the primary ingredient of liquid bleach) and $C_6H_8O_7$ (citric acid) was successfully used to polish a variety of III-V semiconductors [6]. When included, the abrasive size and concentration both play a role in the final surface quality [11]. Overall, the factors of the slurry which influence the CMP results are the liquid (elements, pH), the solid (size, concentration, material), and the flow rate of slurry onto the pad.

Further mechanical contributions to CMP are made by the carrier and the pad, which is attached to a platen (a very flat surface). This platen/pad combo shall be referred to as a "plate" throughout this work. As shown on part (b) of Figure 1, the plate in this CMP style rotates around its center and can do so with a variety of rotational speeds. The pad itself is made of a porous polyurethane [12] with a given hardness, depending on pad model. A harder pad will more reliably etch a harder sample, while a softer pad will avoid over etching [12]. During polishing, the pad will absorb and distribute slurry, and respond to these chemical interactions, as well as respond physically to the contact with the sample carrier. Since these interactions will cause the pad to shift in quality over the course of a polishing run [13] [14] [15], a conditioner is used before hand to bring the pad to a starting baseline which, ideally, can be maintained through the polishing. The plates contribution to CMP is therefore in pad material

(hardness, porosity), the plates rotational speed, and how the pad has been conditioned before the start of CMP.

The final essential components of the CMP are the conditioner and the sample carrier. These two components operate, mechanically, in a very similar way, but have a few notable differences. The conditioner is a brush head, while the sample carrier is ring of rubber with cutouts for inserting the sample into. To allow for global uniformity of a sample, the sample carrier has the possibility to have a back pressure to the carrier surface, which lets the surface hold a concave, convex or flat surface depending on need. Apart from these differences, the conditioner and carrier operate in the same way. As Figure 1 shows, in the CMP used throughout this study, the conditioner is held in the same type of retainer that the sample carrier is, though this can vary among other CMP styles. Both can have their speed along a reciprocation motion modified, as well as have this sweep range defined (can sweep across any continuous portion of the pad along one radius). The carriers themselves have a modifiable rotational speed as well as "download", with indicates with what pressure the carrier will push against the plate. The parameters of note for the carriers are thus back pressure (flatness), download (pressure against plate), carrier speed (rotational), sweep speed and range.

Some of these parameters are easier to change in situ than others. The pad must be installed before CMP is commenced, and therefore cannot be altered during the run. The slurry can connect to one of four dispensers, and so can be altered during the run, so long as the varieties of slurry are present. Most easily modified are the values controlled by an attached computer, which runs the CMP. These are the sample and brush carrier speeds, downloads, backpressure, sweep speed and range, as well as the plates rotational speed, and the flow rate of the slurry. All these parameters can be modified relative to one another and in conjunction with one another. Predefined steps can be written, along with how long they should be performed for, and so various combinations of parameters can occur in one run when compiled into a recipe.

2.3 Surface Topology Measurement

AFM

AFM (Atomic Force Microscopy) is a scanning probe microscopy technique with high resolution. AFM maps the surface of a sample by raster scanning an ultrasharp tip across the surface of interest in one of two main modes: contact or tapping. Contact mode brings the AFM tip, which is placed on a flexible cantilever, into contact with the surface and drags it across the sample, while the system attempts to keep it in contact. When the tip reaches a "hill" on the surface, the cantilever bends and the tip is moved upwards. When reaching a "valley" the same happens but in a downward direction. To determine how much the cantilever has bent (and thus how much the tip has risen/fallen) a laser is bounced off the back of the cantilever onto a four-quadrant photodetector, depicted in Figure 2. It is calibrated such that on a smooth surface, the laser will shine equally in all 4 quadrants, and so when the bottom two detectors have a higher intensity than the lower two, the tip has moved down, and when the top two read more light, the tip has moved up. Using a PID controller, this deflection leads to a Z-piezo to retract or lower the tip so as to keep a constant force on the surface, and this z-piezo reading is what is read as the local sample height. The tip is raster scanned along x and y axes, recording this z height at each coordinate. These can then easily be displayed as a colormap, or even plotted in three dimensions.

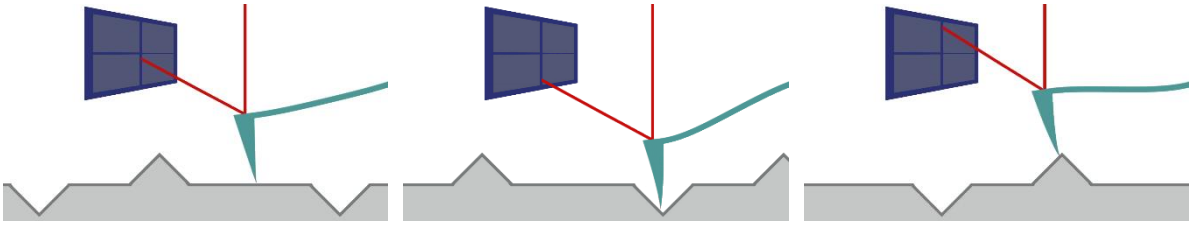

Figure 2: Schematic of AFM. As the tip is dragged across a valley, the cantilever bends, lowering the laser. As it climbs a hill, the laser is raised.

Contact mode has a few drawbacks, however, particularly for softer, dirtier samples. By dragging the tip across the surface, the surface can be damaged [16]. This would mean that any surface damage imaged could not be ruled out to having been caused by the AFM. In contact mode, the tip also has a tendency to collect loose particles on the tip as it scans [16]. This leads to a larger tip, which will now deflect more and more as it collects more loose particles. For these reasons, tapping mode was created, and it shall be the mode used in this study. In tapping mode, the tip oscillates up and down in some user defined range. The tip as it taps along a flat surface is taken as the default oscillation amplitude. When a "hill" is reached, the oscillation is cut short, and the amplitude decreased. When a "valley" is reached, the oscillation is less impeded, and the amplitude increases. The same PID-controller uses the Z-piezo to return the tip to its default oscillation, and this delta z is recorded as the sample height. Tapping mode has its own potential drawback from this recoil-based measurement system. If part of the sample is a harder material, and part of the sample is a softer material, the recoil in these regions will behave differently than one another [17]. This can lead to an inaccurate height reading if the regions are not well defined. In this study, however, the whole of the sample to be studied (apart from any impurities) shall be InSb, and so this drawback is avoided. In both modes, minute adjustments to scan location can be made using the x and y piezos and both can be done at ambient pressure, allowing for relatively quick scanning of multiple samples.

Profilometer

The profilometer operates in a very similar fashion to AFM's contact mode. Typically, a profilometer uses a stylus with a sharp tip to trace along a sample. The stylus comes into contact with the surface and traces along the surface, most commonly along a single line, though the tool can also measure in single points, or do raster scans to map a 2D surface. The tip aims to exert a constant force with the surface, and so when the tip comes to a point which is lower than previously, it will lower until a force is applied to the surface again, and when the tip reaches a point which is higher than previously, it will retract a bit to reduce the force between the tip and surface. In this way, the height along the line can be recorded with great accuracy, so long as the feature sizes are at least as large as the stylus tip. The major utility of the profilometer is that it can be operated quickly and easily. Being able to run at ambient pressure allows for the quick study of many samples in series. Profilometer also can operate over the scale of cm instead of just μm like the AFM, leading to it being a better tool when scanning a whole sample, or when there are steep height differences in the sample.

3 Experiment

3.1 Setup

The most important piece of equipment used in this study is the Chemical Mechanical Polisher. The model used is a Logitech Orbis CMP and is shown in Figure 3.

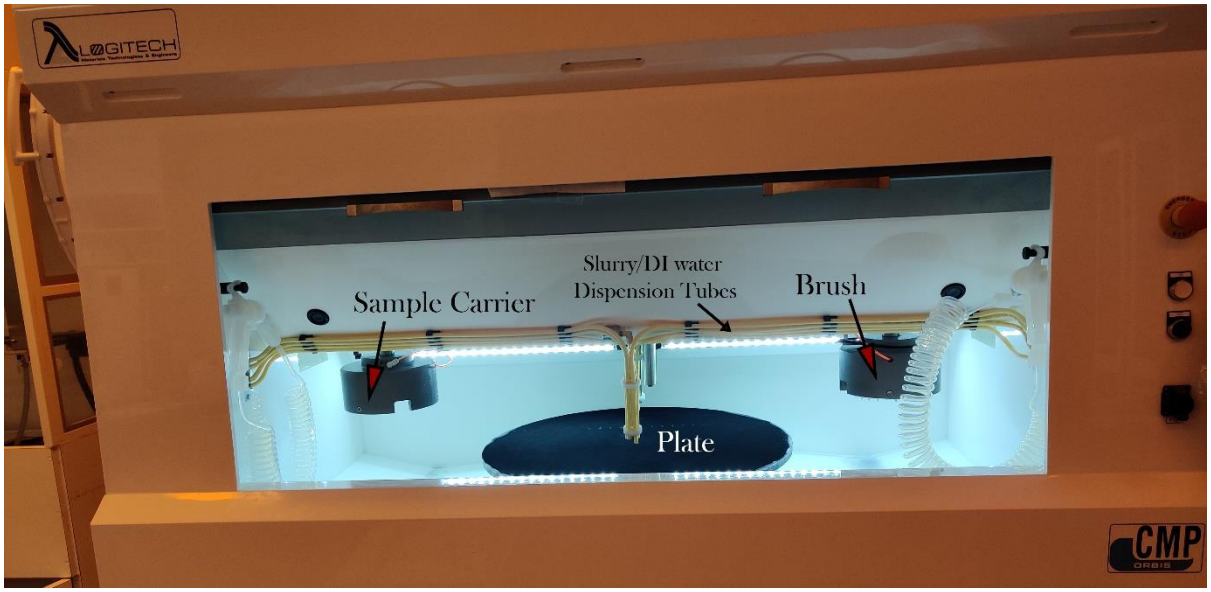

Figure 3: The CMP used in this study.

It can be seen that the main components of the CMP are the two carriers (one to carry the sample and one to carry a brush), the plate, and the slurry tubes. The brush and slurry tubes help to prepare the plate before polishing occurs, and during polishing, the sample carrier makes contact with the plate while a flow of slurry is fed into the system. To mount a sample to the carrier, a sample holder (shown in Figure 4) is used. This sample holder is specific for each size of sample, meaning that one type of holder will need to be used for 8 mm x 10 mm chips, and another would need to be used for 4-inch wafers. The sample holder is easily removable from the CMP and so any standard size of sample can be accommodated (to an upper limit of the size of the carrier).

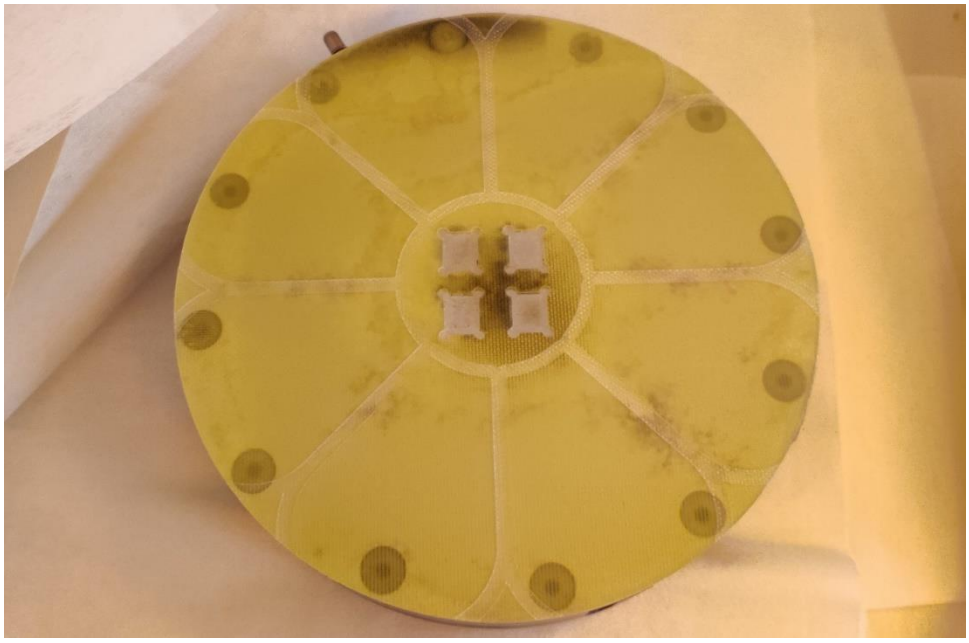

Figure 4: Sample holder for 8 mm x 10 mm chips.

For polishing to occur, the sample must have an "overhang", which means that the sample must come up above the sample holder's surface as show in Figure 5. This is done with shims and a NAPCON. The shims are small objects in the shape and size of the sample holder cutouts which serve to lift the sample higher up. They are color coded based on their thickness. The NAPCON is like a shim, but it has a rough surface which helps keep the sample from falling out of the holder. The NAPCON is always used. The total thickness of the shims, sample and NAPCON should put the surface of the sample about $50\ \mu m$ above the surface of the sample holder.

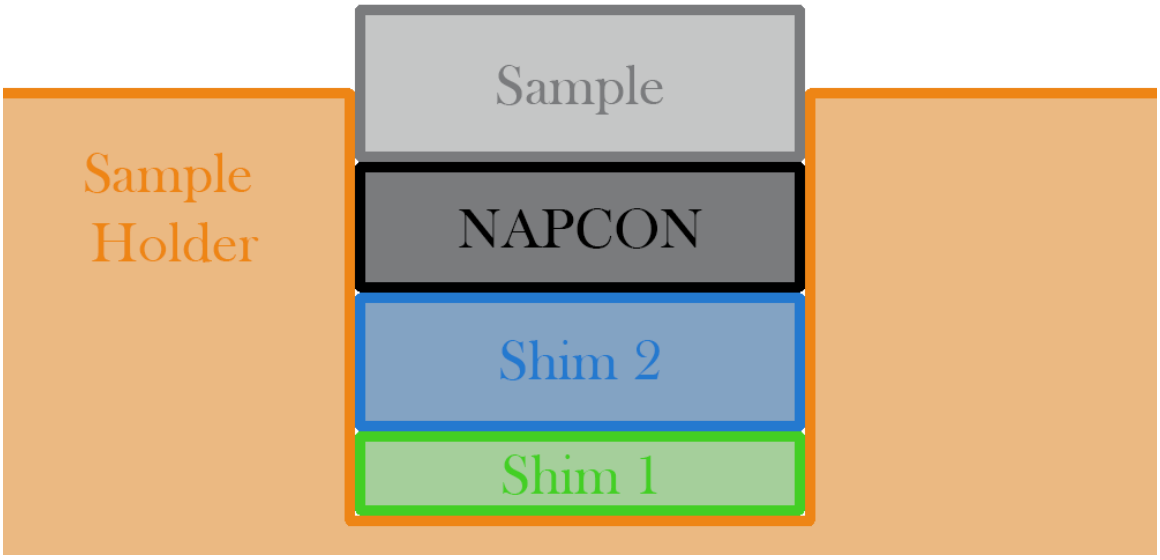

Figure 5: A schematic of how a sample can be "shimmed" to achieve an overhang.

After the samples were polished, they were studied using a Bruker DektakXT stylus profilometer, Bruker Icon AFM, and an optical microscope.

3.2 Preparation of Sample

In order to compare the polishing qualities of the different CMP variables, it is important to have a consistent starting point for each sample polished. To ensure this, chips were made from the same wafer of InSb and run through the same preparation procedure. First, the chips were soaked in acetone for 5 minutes and then IPA for 1 minute before being cleaned in an Oxygen Plasma asher for a further minute. Once cleaned, the chips were baked for 1 minute at 95 ℃ before being spin coated with the negative resist MAN-440 at 6000 rpm for 60 seconds. They were then baked a further 3 minutes at 95 ℃ to set the resist, leaving them looking like part a of Figure 6. It is important to use a negative resist because of the undercut it creates, assisting the subsequent lift off process. The resist-coated chips were then exposed to hard contact for 5s+50s in a UV mask aligner, as seen in part b of Figure 6 where the undercut formed in the negative resist can be seen. After UV exposure, the chips were developed using MAD-532 for 105 seconds and then rinsed in DI water for 60 seconds. This left the chip coated with hardened resist in some regions, while other regions left the InSb substrate exposed, as part c of Figure 6 depicts. These holes were later etched (part d of Figure 6) using a dry etcher and the chemicals CH_4, H_2, and Ar at 110 ℃ for 7 minutes. This gave an etch depth of approximately 500 nm though this was verified later using the profilometer. These holes were then filled with tungsten using a sputter tool, so that 40 nm tungsten was deposited. This is shown in Figure 6, part e. Tungsten lift-off was then performed by soaking the chips in Acetone heated to 60 ℃ for 30 minutes. The resist then fell off, leaving the chips with holes in the InSb with a layer of tungsten at the bottom which are ready for polishing, as in Figure 6 part f.

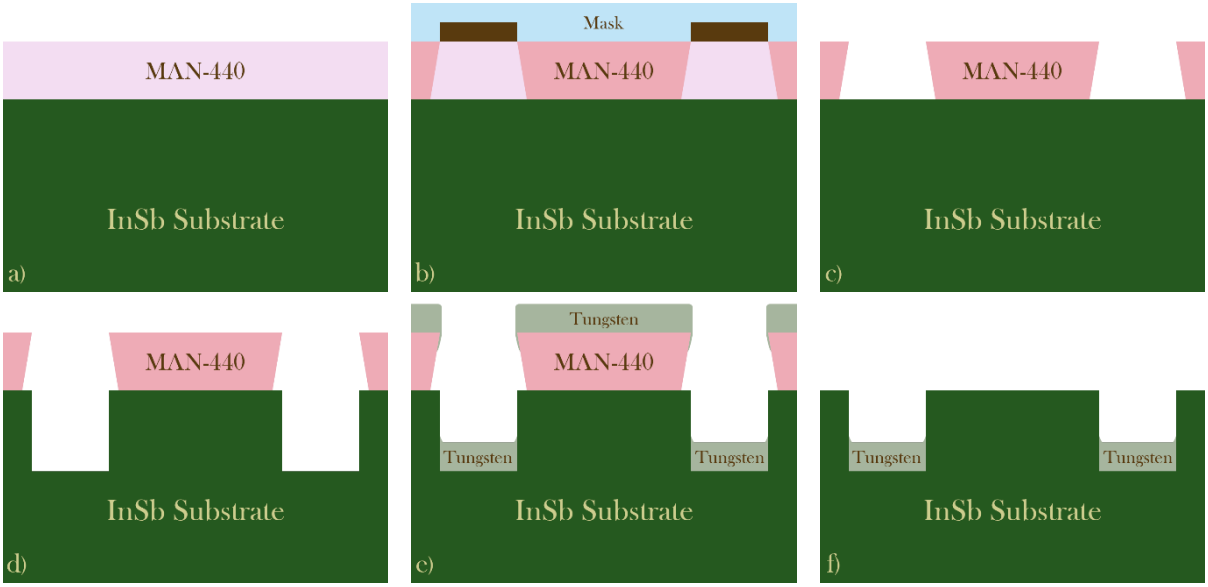

Figure 6: Schematic of sample processing steps taken. a) shows the InSb substrate as well as the negative photoresist. b) the photoresist is exposed to UV light, and the exposed regions harden. c) the unexposed regions are developed away. d) the unexposed regions are dry etched. e) Tungsten is sputtered onto the sample. f) the remaining resist is lifted off, along with the tungsten on top of it, leaving the finished sample.

The holes in the sample are important for having a consistent reference point to which the height of the InSb can be measured to determine the etch rate of each specific CMP run. By

measuring the depth of the holes before polishing and after polishing, the amount of InSb etched per minute can be easily determined.

To polish, a slurry is needed. It has been shown that a mix of $NaOCl:DI(1{:}10)$ + $C_6H_8O_7:DI(1{:}2)$ is sufficient for polishing other III-V materials [6], and so this mix was selected for use as the slurry in this work. When polishing, there are several variables which affect the result of a CMP run. The carrier can have its speed and sweep range specified, as well as its rotational speed. The carrier can also have its download (the pressure it presses against the plate with) and back pressure (a pressure which can make the carrier concave, flat, or convex). The plate itself can have its rotational speed modified, and the flow rate of the slurry can be selected. All of these variables can be selected in any desired permutation across any necessary number of steps. With limited samples and limited time, the parameters of study were limited to those which seemed most likely to have a large effect on the samples: carrier download, plate rotation speed and carrier rotation speed. The backpressure was held at a constant 25.0 PSI (to maintain a flat surface), while the sweep speed and range were both held at 100%. With the exception of Sample 1 (which was polished for 3 minutes straight), the polishing time for samples 2-7 was the same: three runs of 60s. The values selected for each of the three variables are shown in Table 1. Sample 1 can be seen as a baseline from which all further samples were permuted from. Sample 2 decreased its carrier speed to its minimum, while Sample 3 decreased its carrier download to the minimum value. An initial assessment of the download's contribution led to further study in Samples 4 and 5, while higher and lower plate speeds were studied in Samples 6 and 7.

*Table 1: Variables modified for each sample during their CMP main step. *3x1 refers to three sets of one-minute polishings.*

	Sample 1	Sample 2	Sample 3	Sample 4	Sample 5	Sample 6	Sample 7
Download Pressure [psi]	0.7	0.7	0.4	0.5	1.0	0.7	0.7
Plate Speed [rpm]	50	50	50	50	50	30	70
Carrier Speed [rpm]	30	10	30	30	30	30	30
Time [min]	3	3x1*	3x1	3x1	3x1	3x1	3x1

3.3 Analysis of Sample

In order to determine the etch rate of the different variables, the profilometer was used after each CMP run. Each sample was studied in a line across all enclosed markers in five general locations, marked on Figure 7 as a, b, c, d, and e. This spread was chosen to get a more concrete comparison of specific regions across runs and over time, as well as to study if the sample was being polished uniformly across the surface. When all polishings for each sample were done, they were studied in the AFM in the regions within the dashed boxes marked as X, Y, and Z on Figure 7. These regions were also selected to allow for sample uniformity checks which

could be compared across samples. To process the data from the AFM, the SPM visualization tool “Gwyddion” and Bruker’s AFM image analysis tool “NanoScope Analysis” were used. The samples were then imaged with an optical microscope, though these locations were chosen to provide the most useful results on a sample-by-sample basis. Certain samples were then cleaned with ultrasonic baths, PVA sponges, or both, and then imaged optically again. The regions of the “post-cleaning” optical images were taken to match the optical images taken for that sample previously.

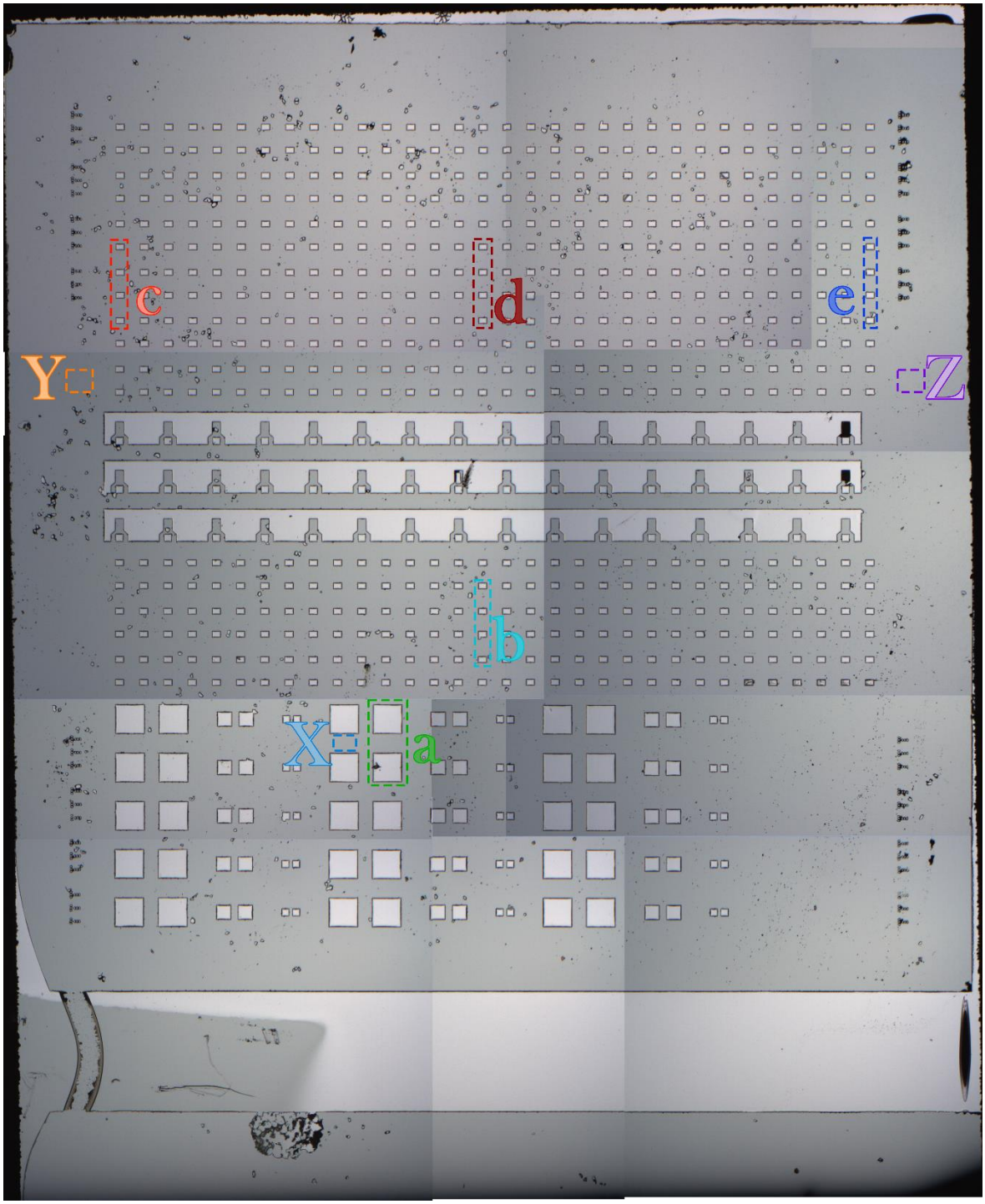

Figure 7: A panoramic overview of an unetched sample taking using an optical microscope. Regions a, b, c, d, and e were studied by profilometer in a line across all enclosed markers. Regions X, Y and Z were studied by AFM in a 2 μm x 2 μm area within the accompanying dashed box.

4 Results and Discussion

4.1 Etch Rate

By comparing the profilometer data for each sample between the consecutive runs, an etch rate can be determined for each set of variables. When the samples are scanned with the profilometer, a plot such as that show in Figure 8 is obtained. In this figure, clear steps can be seen, with the flat top regions being the InSb surface, with the lower regions being the W coated troughs (the lighter colored features in the sample overview). To illustrate, the profilometer data would have traveled along some of the large squares, such as the green line in the right of Figure 8.

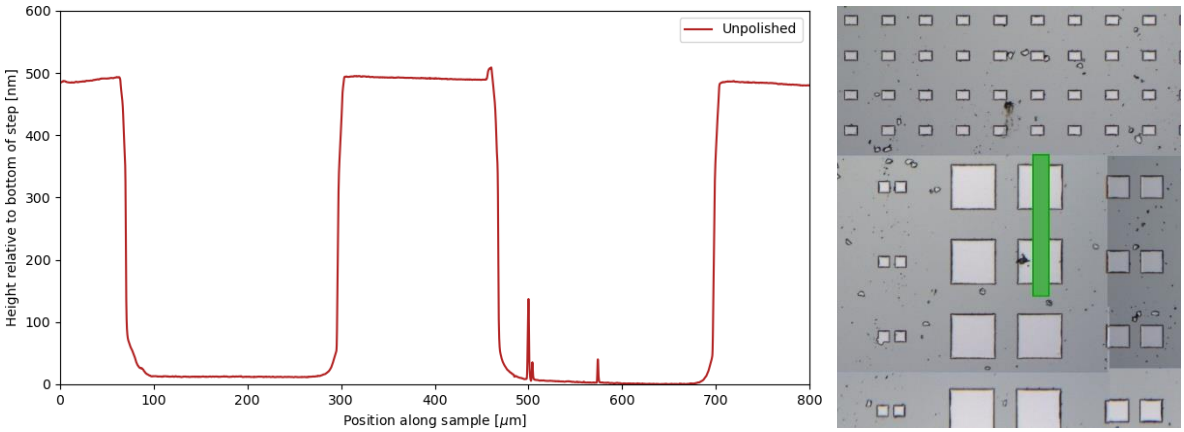

Figure 8: Profilometer data taken of an unpolished sample, along with an overview of the sample with the region studied (region a) in the profilometer marked in green.

The depth of this interface can be measured, and then compared to the depth in subsequent runs. In Figure 9, further profilometer measurements have been overlayed with the measurement from Figure 8, where a couple observations can be noted. Firstly, the height of the interface is noticeably decreasing. This indicates a clear etching, and an etch rate per minute can be extracted from this change.

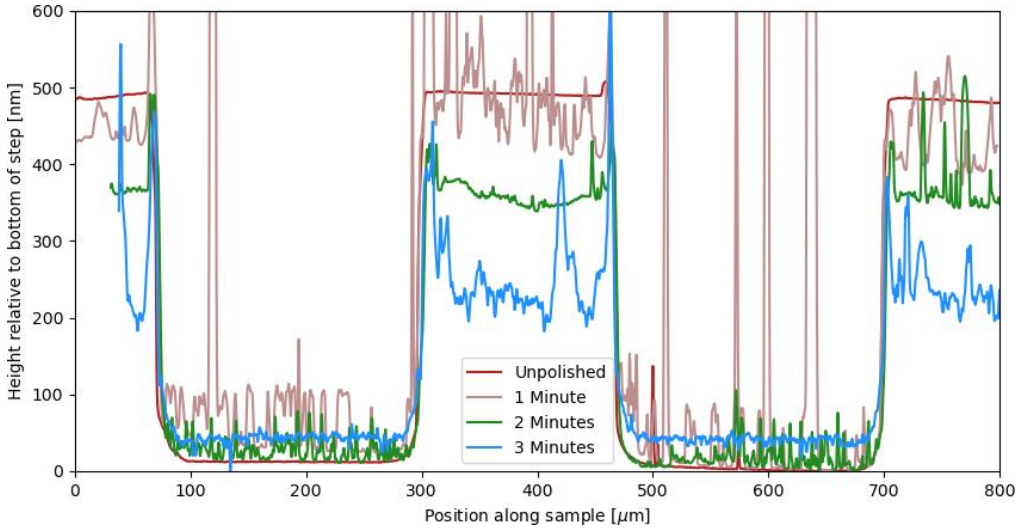

Figure 9: Profilometer data of region a of a sample when unpolished and polished for 1,2 and 3 minutes.

Secondly, the surface is noticeably rougher than previously. As this project is devoted to making the surface of InSb as smooth as possible, this is a bit of a backstep. This roughness

could come in two possible forms: the InSb surface itself could have become rougher, or else there could be some debris on the surface which makes the sample rougher. Which of these two options is most likely will be studied later on using AFM measurements and cleaning methods. The introduction of roughness in the tungsten coated floor regions (which do not make contact with the polishing pad) is, however, a strong indication that particle contamination contributes to at least some of this roughness.

Even without knowing the source of the surface roughness, the etch rate consistency for the variables used can be determined. Plotting the depth of the features relative to the unpolished samples gives the graphs in Figure 10.

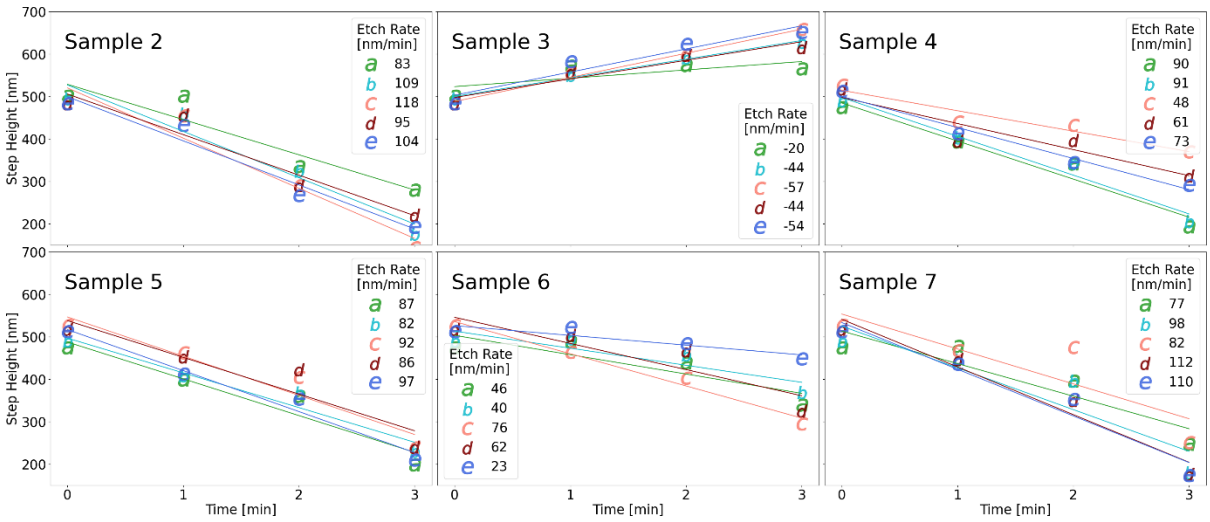

Figure 10: Etch values for each of the non-baseline samples across each of their three, 1-minute runs. The a, b, c, d, and e markers refer to the region of the samples where the measurements were taken, as shown in Figure 7.

By plotting a linear regression between height values in each region, the etch rate per minute can be determined, and compared, as in Figure 11. In these plots, the range shown indicate the etch rates in the regions denoted in Figure 7. A smaller box means that the etch rate is rather consistent across the whole sample, while a larger box denotes the opposite. The two most consistent samples, in terms of etch rate, are Sample 1 (0.7 download and 50 plate speed) and Sample 5 (1.0 download and 50 plate speed).

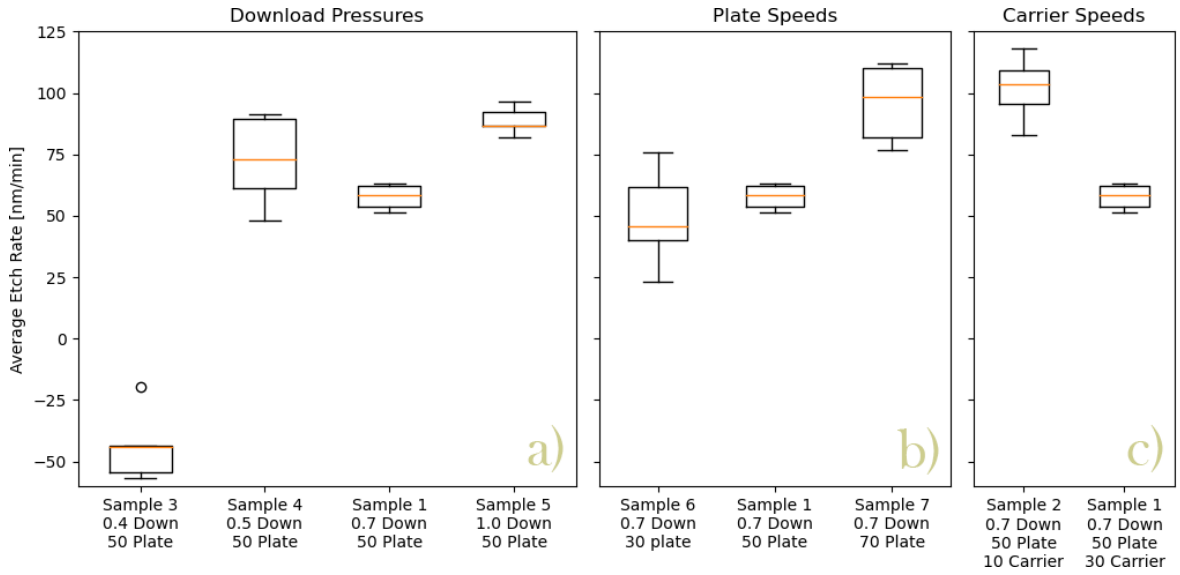

Figure 11: Etch rate per minute of each of the 7 samples. a), varying downloads b) plate speeds, c) carrier speeds.

Sample 1 was the only sample to be polished for 3 minutes all at once, and therefore suggests that single, longer polishing runs are more consistent than multiple shorter runs. Sample 5 has the greatest contact force between the sample and polishing pad, suggesting a high download is important in sample wide etch uniformity. Interestingly, Sample 3 (0.4 download and 50 plate speed) appears to have grown thicker. Several possibilities exist for how this could happen, though some are more likely than others. It could be the case that a low download polishes so little of the surface that any debris which collects on the surface will make it appear as though the surface has grown. This would require quite a broad coverage of debris at least 150 nm in height to be deposited. This can possibly be tested for by cleaning the sample, which will be shown further on in the results section. It could also be that the W toughs are somehow affected or even removed during the process thus our assumption of a constant unchanged reference height is invalid. This would be more difficult to check with profilometer alone, as some objective measurement reference is needed for comparison, and so some other measurement techniques must also be performed. It can be seen from the data in Figure 11 that, with the exception of Sample 3, the download pressure used does not influence the average etch rate much. The global uniformity (how similar the etch rate in each of the five regions was) increases considerably, however, with an increased down pressure. Increasing the plate speed shows the inverse of increased download pressure: the global uniformity appears unaffected by plate speed, while an increased plate speed noticeably increases the etch rate. Changing the carrier speed to its minimum appears have slightly increased the average etch rate, though more tests would be needed to make certain.

4.2 Sample Cleanliness – Nanoscale

As the profilometer data indicated the samples becoming rougher after polishing, it was of interest to check the sample on the scale of micrometers. This, in theory, should allow for the analysis of the surface while ignoring any surface contaminants. Useful to this end is atomic force microscopy (AFM), which can easily allow for the 3D mapping of $2\ \mu m\ x\ 2\ \mu m$ regions of each sample. Once analyzed by AFM, the surface of a clean, unpolished sample looks like Figure 12.

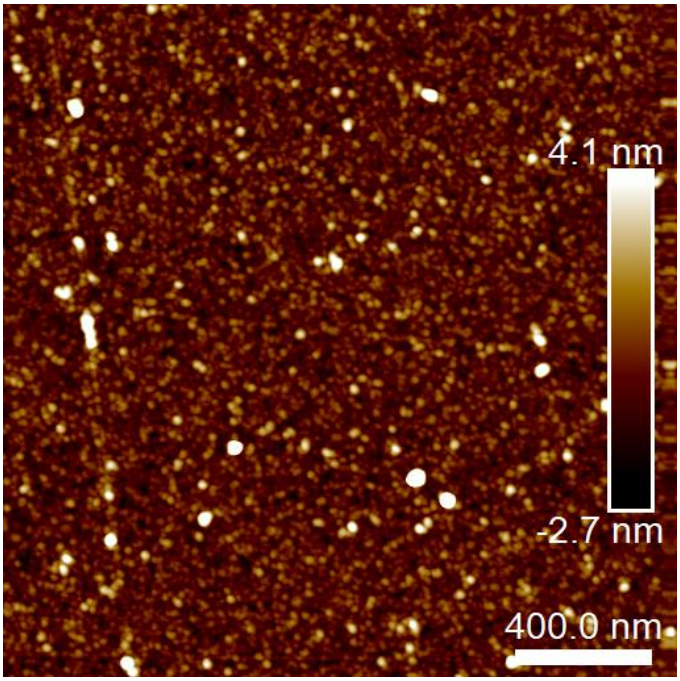

Figure 12: AFM image of a region of an unpolished sample.

Once polished, however, each sample becomes more contaminated by external particles, though to varying degrees. Sample 7, for example, was one of the cleaner samples and came away with regions looking more like Figure 13. Note while the surface of the unpolished sample looks rougher at first glance, this is due to the significantly different color scales in the two images.

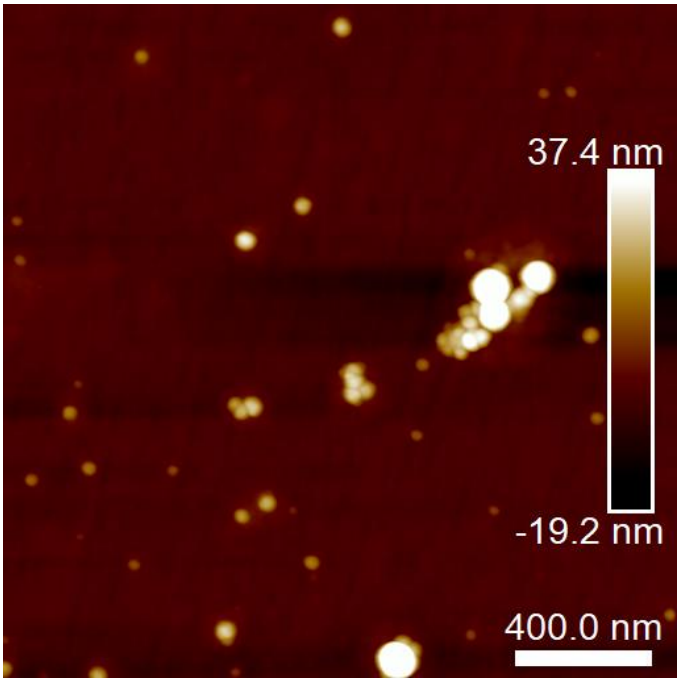

Figure 13: AFM data of a relatively clean Sample 7.

Each bright spot here in Figure 13 is assumed to come from a particle that was left on the surface after polishing. It can also be seen that the particles can group up to form larger particles. This grouping will be discussed when considering the best method for polishing. Also

note the black streaks to the left and right of the largest particle groups. These are simply artifacts from the left to right scanning that the AFM does (verifiable by changing the scan axis) and is not any surface scaring caused by the particle group.

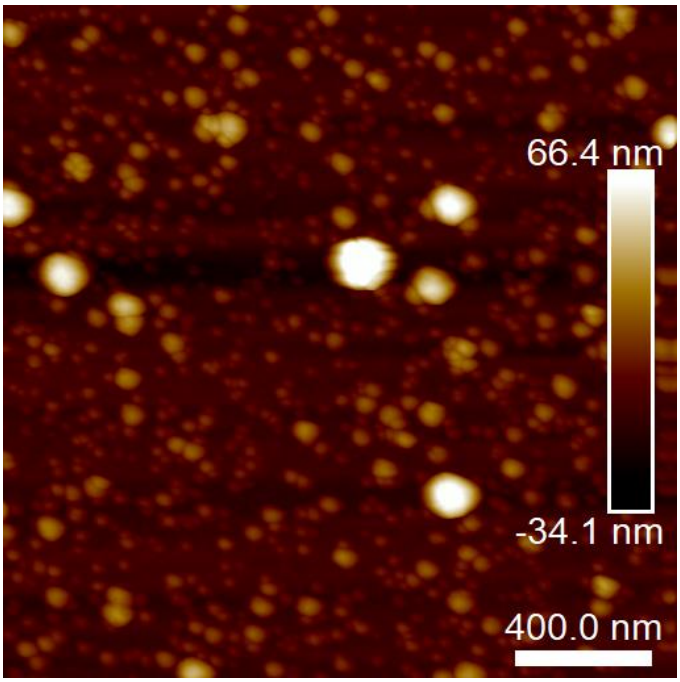

Figure 14: AFM data of a very dirty region of Sample 3.

In Figure 14, a very dirty region of Sample 3 can be seen. There is very little clean surface available, which complicates the qualification of the roughness between particles. Most regions of most samples are more similar in dirtiness to Figure 13 than to Figure 14, but it is interesting to note that Sample 3 has regions this dirty, especially when looking at the sample from a macro perspective, as will be done shortly.

First, however, it is relevant to quantify the dirtiness of each sample, so as to have an objective point of comparison between them. To do this, the peaks made by the particles were isolated using the analysis tool Gwyddion, and then the number of peaks were counted, and their total area recorded, giving the result in Figure 15.

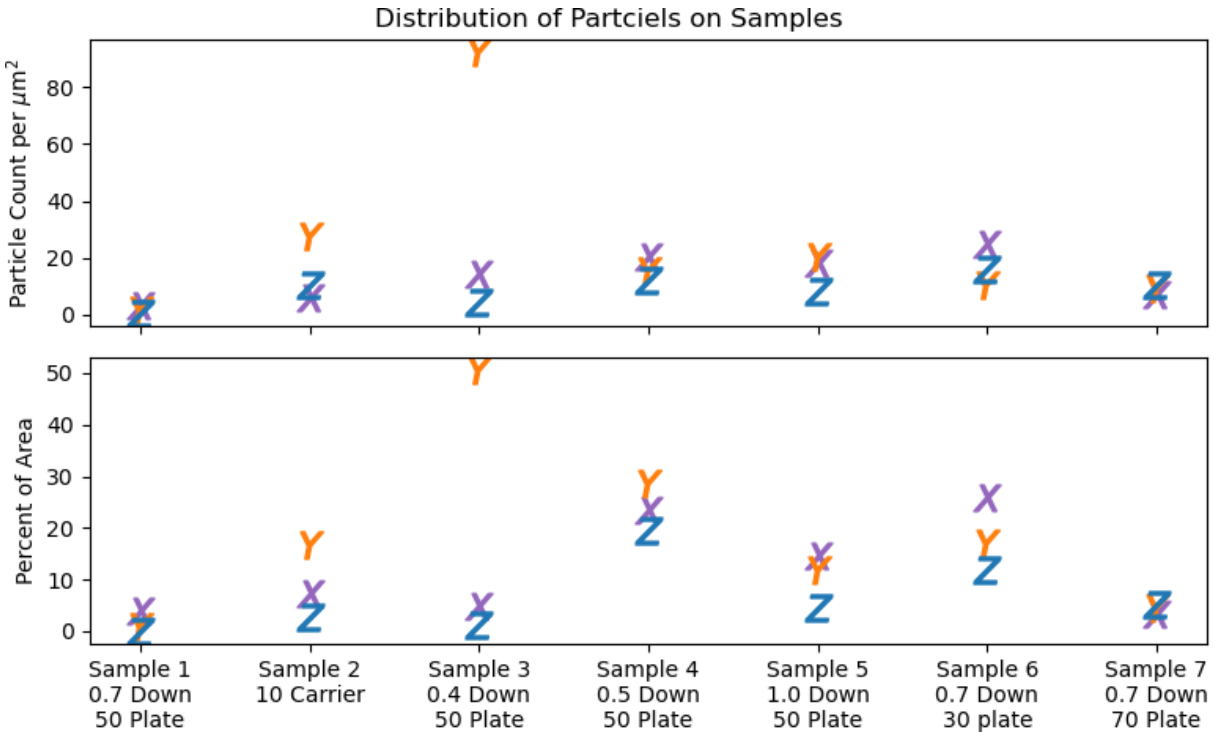

Figure 15: Particle count (top) and total particle area (bottom) of each of the 7 samples. On the left, the varying downloads are compared, in the middle, the plate speed, and on the right the carrier speed. The X, Y, and Z markers refer to the region of the samples where the measurements were taken.

Again, Sample 1 has an advantage here, being the most consistently clean sample, suggesting single runs are better than multiple runs. Most likely if the samples had each been cleaned after each of their CMP sessions this difference would reduce. Sample 3 is again an outlier in that it has two of the cleanest regions, despite that it also contains the dirtiest region. All told, of the samples polished for 3 x 1minute runs, Sample 7 (0.7 download, 70 plate speed) comes out the cleanest, despite not having gone through any cleaning steps.

4.3 Sample Roughness

Of course, creating clean InSb surfaces isn't the goal, but smooth ones. Unfortunately, having dirty regions complicates the collection of roughness data for whole regions, but it can be found by taking smaller roughness measurements away from the particles, and then finding the distribution of these measurements, as shown in Figure 16.

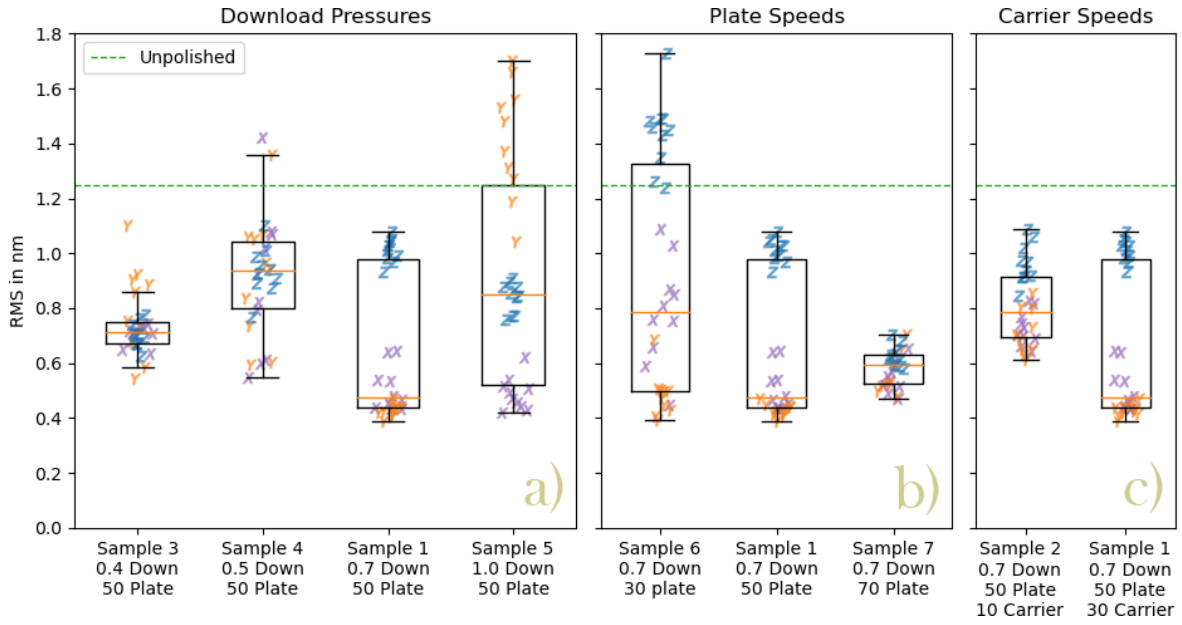

Figure 16:RMS roughness values of each of the 7 samples. On the left, the varying downloads are compared, in the middle, the plate speed, and on the right the carrier speed. The X, Y, and Z markers refer to the region of the samples where the measurements were taken.

Sample 1 no longer has such a clear advantage when comparing surface roughness. Here, the ideal sample will have a low mean value, as well as a tight spread of points. The sample with both of these qualities is Sample 7, which also had the least dirty surface, at least on the nanoscale. The data in Figure 16 appears to show that a lower download pressure provides a smoother, and more consistent surface. A higher download pressure has the possibility of providing a smooth surface, but the consistency across regions is poor. Shows the same trend as download pressure, but with lower plate speeds being comparable to higher download pressures, and vice versa. While the Y regions in all variations of plate speed are comparably smooth and tightly distributed, decreasing the plate speed sees the roughness of the Z and X regions to rise, though they remain relatively tightly grouped around their own means. A decreased carrier speed appears to give a more consistent roughness across regions at the expense of increasing the mean roughness. More data points would be needed to definitively state a relation, however.

4.4 Sample Cleanliness – Global Scale

Particle contamination doesn't only occur on a $2 \times 2\ \mu m^2$ area, however, and the samples must be seen from a more global view as well. The view of the 7 samples from an optical microscope shall follow on pages 18 - 21.

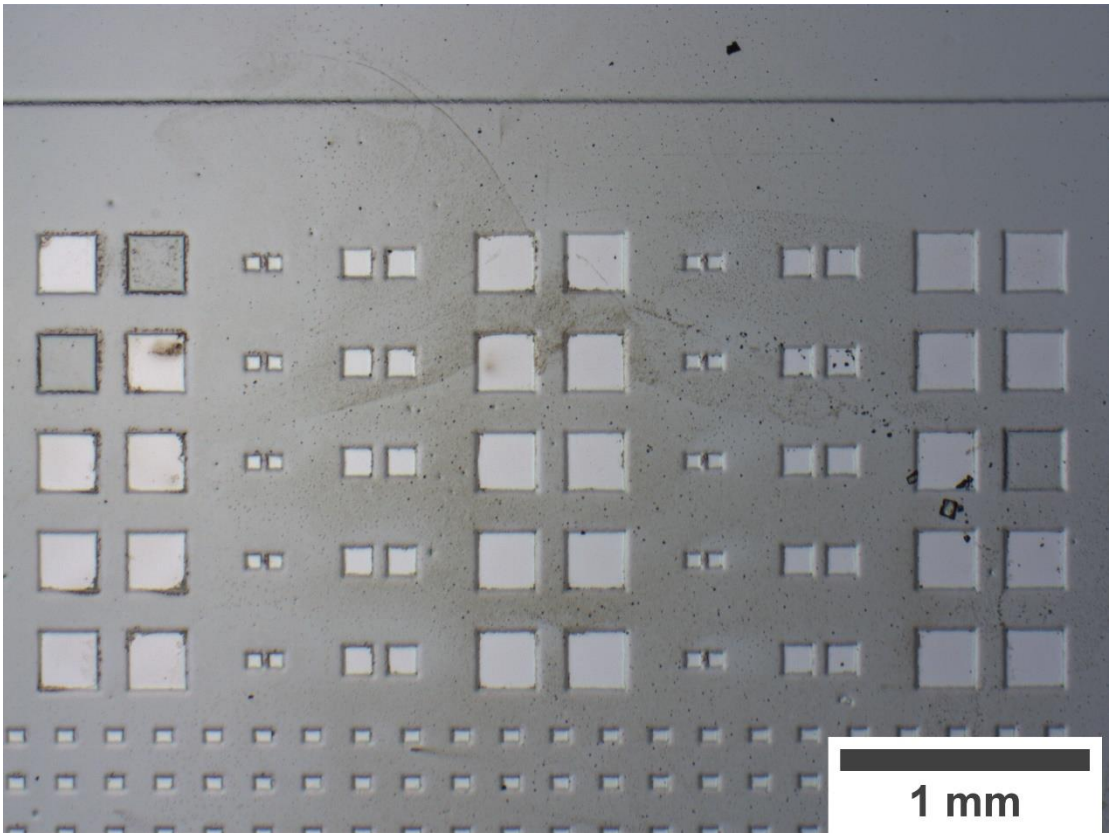

Figure 17: Sample 1 when examined under an optical microscope.

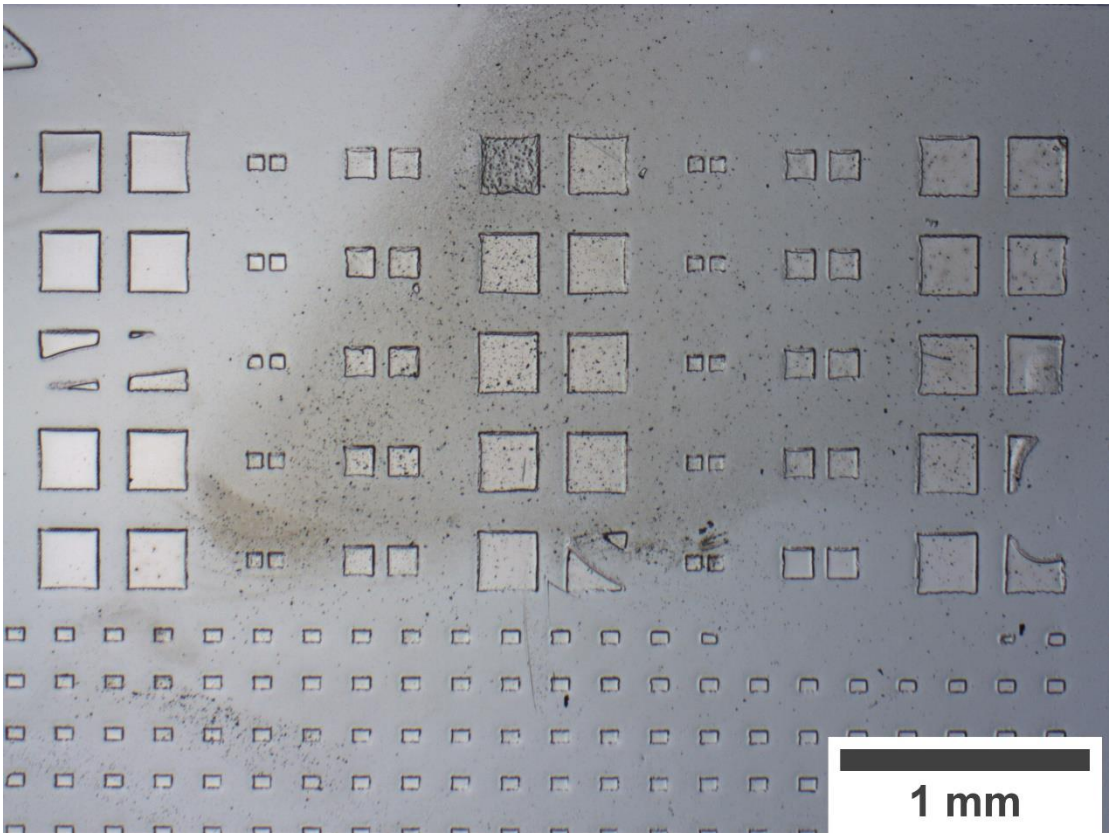

Figure 18: Sample 2 when examined under an optical microscope.

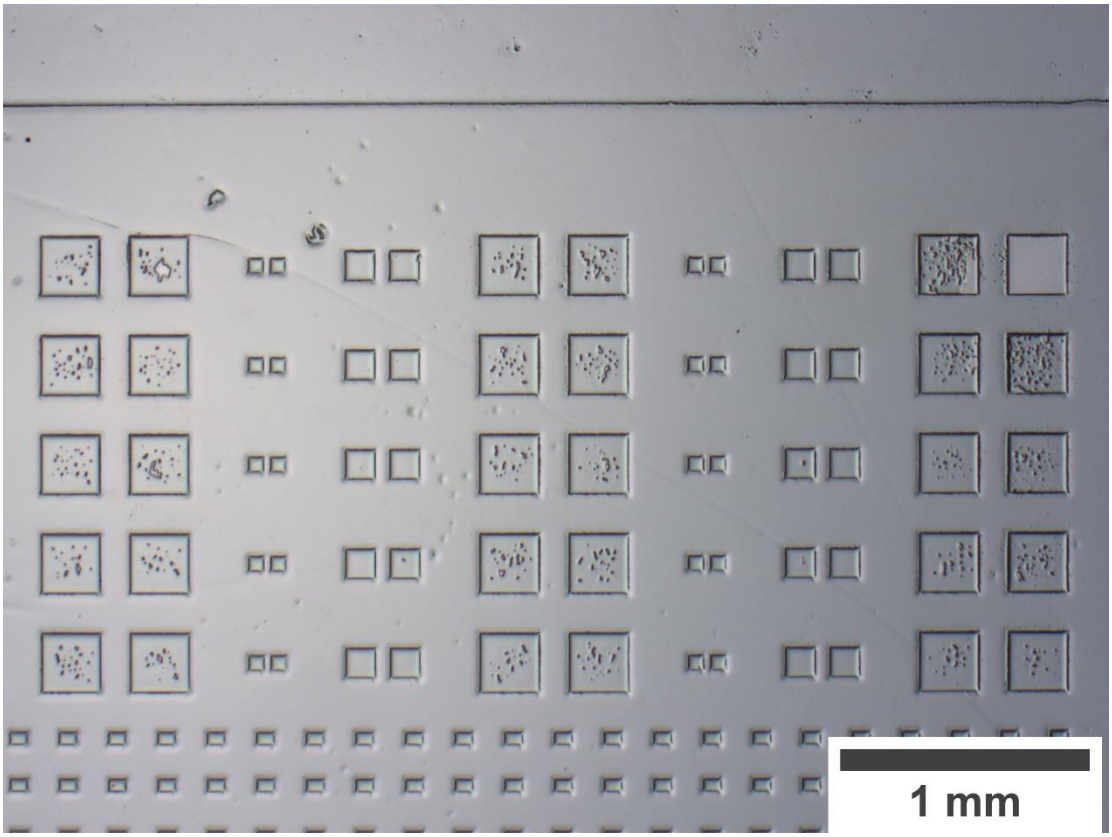

Figure 19: Sample 3 when examined under an optical microscope.

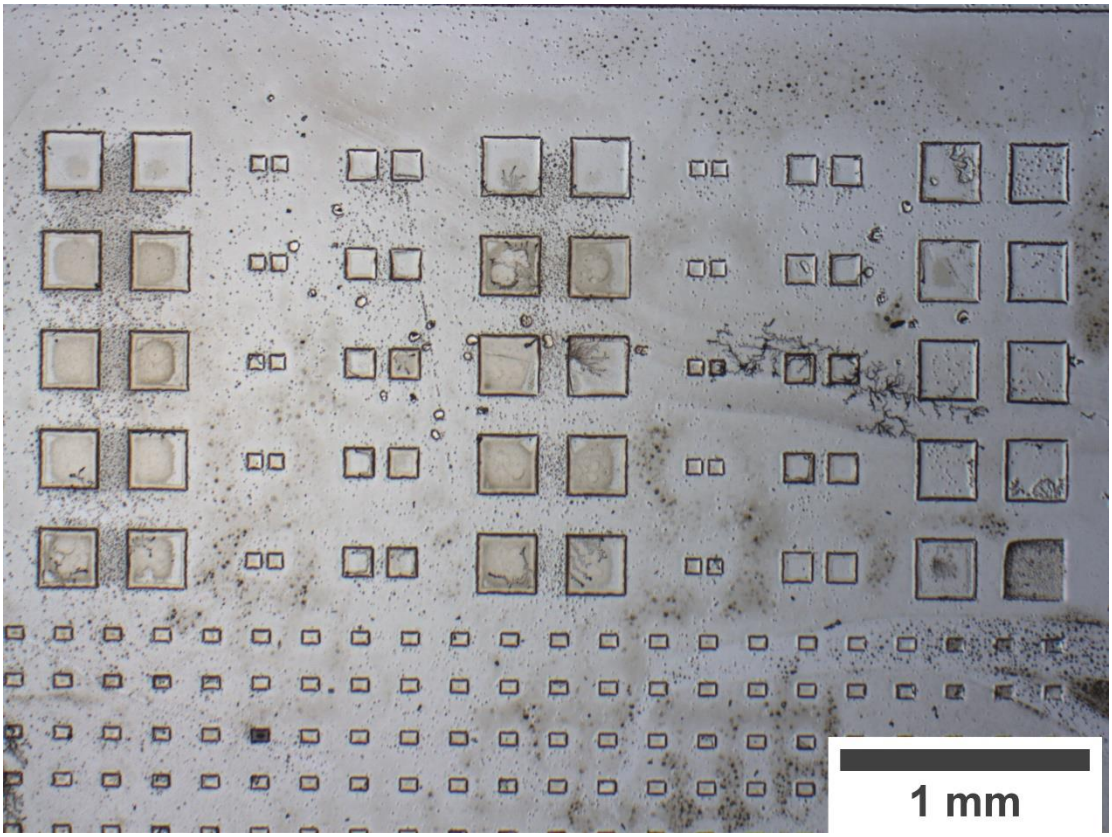

Figure 20: Sample 4 when examined under an optical microscope.

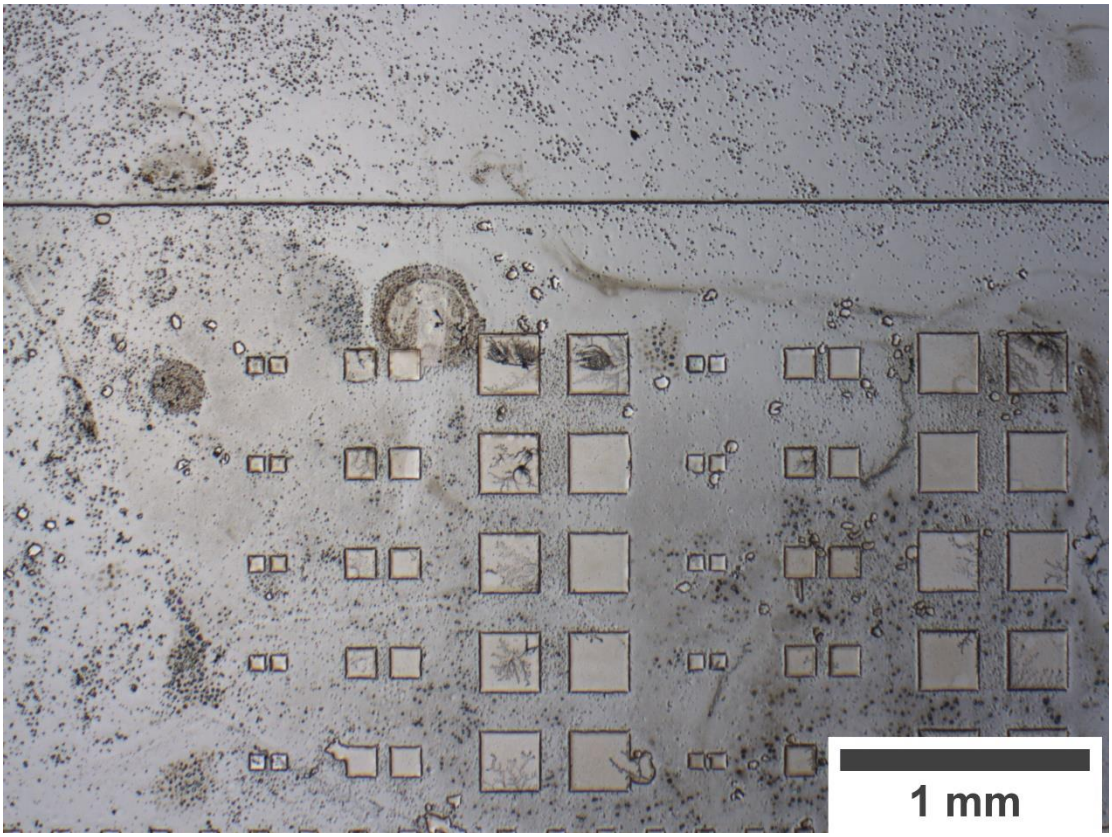

Figure 21: Sample 5 when examined under an optical microscope.

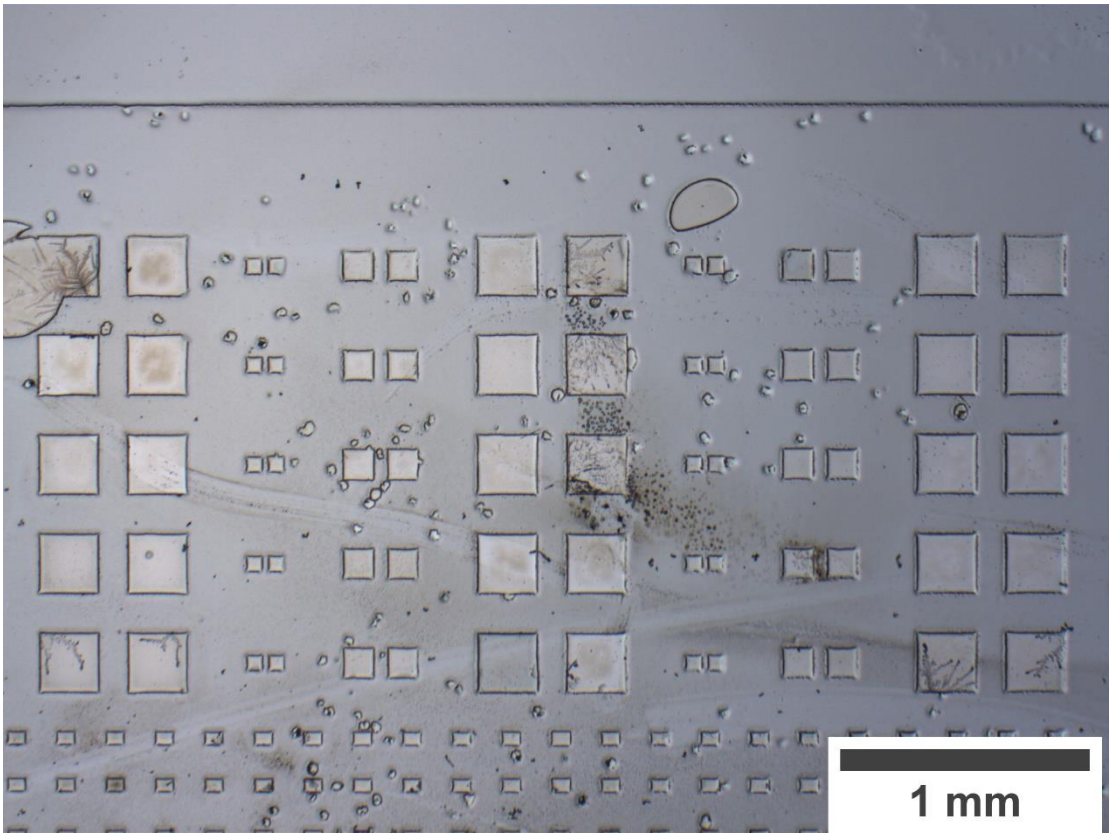

Figure 22: Sample 6 when examined under an optical microscope.

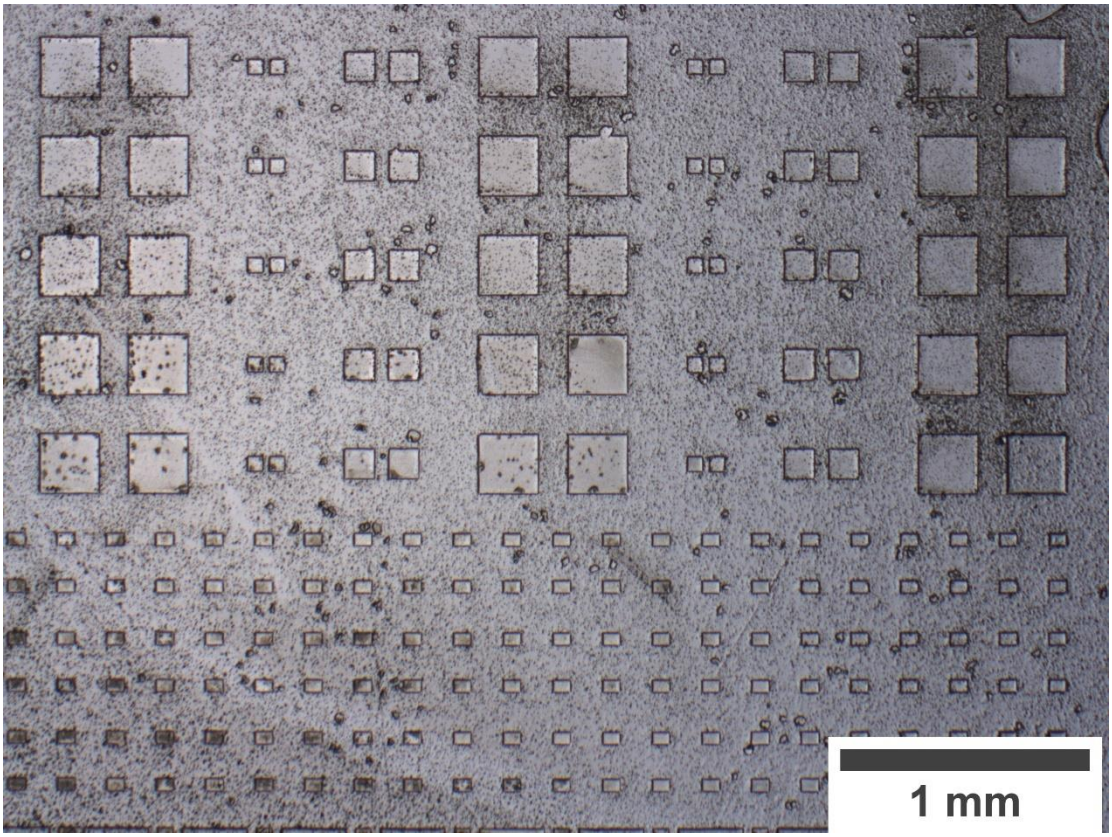

Figure 23: Sample 7 when examined under an optical microscope.

To the eye, Sample 3 in Figure 19 appears to be the cleanest sample, while Sample 7 in Figure 23 appears to be the dirtiest sample; quite the opposite impression from that given in Figure 15. Without a chemical analysis, the source of these particles cannot be determined with certainty, but as the color of the particles is rather much darker than the InSb regions and the W regions, those two materials can be ruled out. It is possible that the particles come from the polishing pad itself, which may be damaged during the polishing. It is also possible that these particles are abrasives from other users' slurries, which have remained in the pad until the polishings done here. With the possible exception of Sample 3 (which mysteriously grew during its polishing) none of these samples are satisfactorily clean enough globally, and so some form of cleaning must be attempted. This cleaning shall be attempted in a very common cleaning method in many fields, being the ultrasonic bath, as well as a cleaning method more common with regards to CMP, namely a clean room ready sponge made of PVA (Polyvinyl Alcohol). PVA sponges are porous and hydrophilic, making them excellent at absorbing excess, water-based slurry along with particles on the surface.

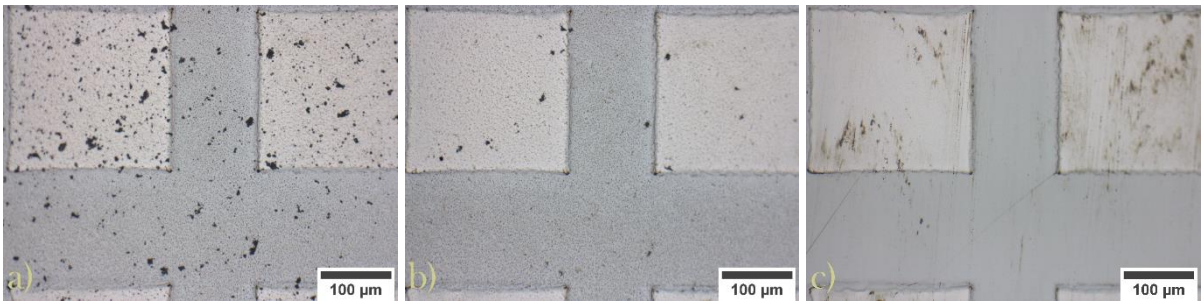

Figure 24: Region of Sample 2 before cleaning (a), after a 5-minute ultrasonic bath (b) and after cleaning with a PVA sponge.

Figure 24b shows the result of putting Sample 2 (in a beaker of acetone) into an ultrasonic bath for 5 minutes gives clear improvements in regard to the largest particles on the surface, but little to no improvement in the smaller particles. The same can be seen across the whole sample. Image c) of Figure 24, however, shows great reductions in the amounts of small particles when using a dry PVA sponge on Sample 2 after it had been submerged in acetone for 5 minutes, then IPA for 5 minutes, then DI water for 30 seconds. It also, unfortunately, introduces some smudging and scratching. The smudging could possibly be cleaned off with a further wiping with the sponge, but the scratching would need to be polished out. This suggests that using the PVA sponge for cleaning requires some fine tuning of pressure and technique to perfect. To get an idea of the improvement the sponge makes to the cleanliness of Sample 2, the profilometer data in Figure 25 can be used. Here the same four squares before using the sponge and after using the sponge are shown, and it is clear that the sponge has been very effective in removing particulates of a few nanometers in height.

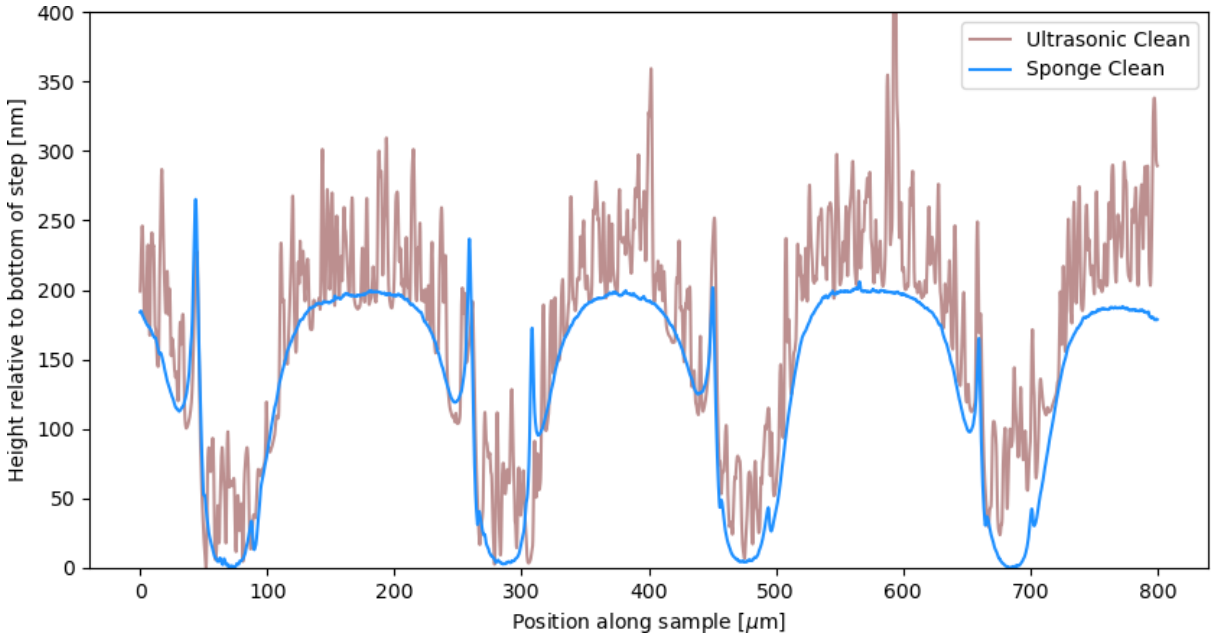

Figure 25: Same exact region of Sample 2 before and after using the PVA sponge to clean the surface.

A further study of methods of using the sponge (sponge soaked in DI water with sample wetted with DI water, sponge dry with sample wetted with IPA, sponge soaked in IPA with sample

wetted with IPA) showed little difference between the four fluid media used. The additional three samples were not, however, run through an ultrasonic bath beforehand, and an attempt was made to use less pressure to avoid scratching. This set of tests can be seen as both a testament to the PVA sponges cleaning abilities in Figure 27, as well as a caution of its limitations in Figure 26.

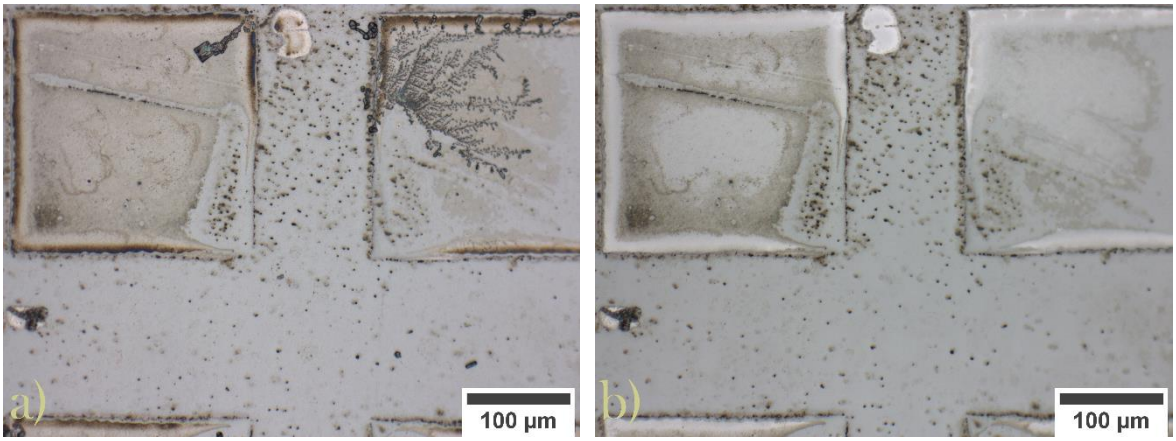

Figure 26: Region of Sample 4 where sponge cleaning has been insufficient. a) is before cleaning, and b) is after.

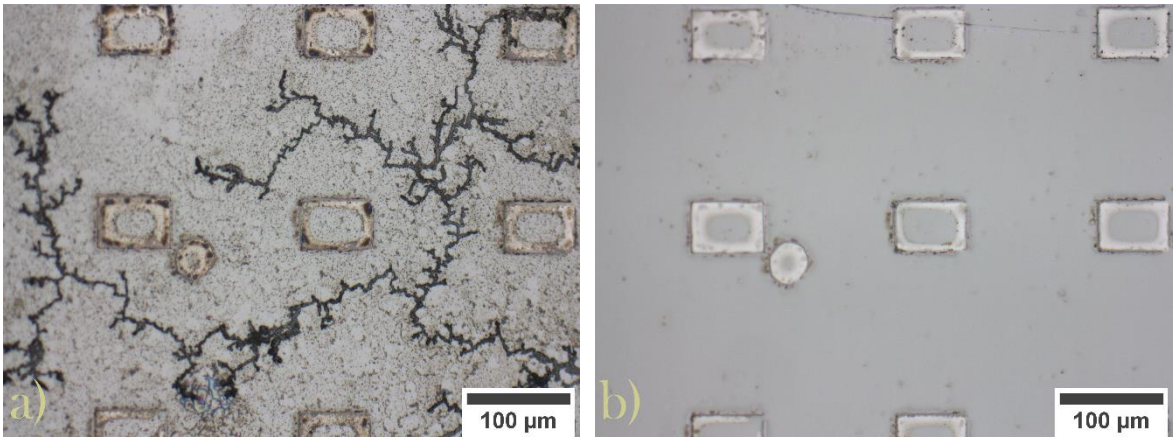

Figure 27: Region of Sample 4 where sponge cleaning has been sufficient. a) is before cleaning, and b) is after.

The sponge does quite well in removing the small particles and fractal compound of particles in Figure 27, but fails nearly entirely in removing the larger particles in Figure 26, though it manages to clean off a fractal there as well. This suggests that while the ultrasonic bath appeared to give minimal benefits in Figure 24, the benefits that it does give fill in gaps where the sponge is of limited utility.

4.5 Final Samples

After considering the various ways in which a sample can be considered desirable, two more polishing runs were conducted to try to combine a good polishing with satisfactory cleaning. The first sample chosen was Sample 3. It had a very clean looking surface in the optical microscope, a clean nanoscale surface in most locations, and a tight, low distribution of surface roughness. Sample 3s main drawback was that it mysteriously grew instead of etching, and this needed to have some sort of explanation. It was hypothesized that if the sample wasn't growing, but instead something was making the W floor regions lower. The second sample chosen to

repeat was Sample 7. This sample was very clean on the nanoscale and had the best distribution of surface roughness values of all the samples. The drawbacks of Sample 7 were that the etch rate was the highest of any sample, and that the surface under the optical microscope appeared to be the dirtiest. This dirtiness should allow for a "worst case scenario" which the final cleaning method must contend with.

Table 2: Parameters for the final two samples.

	Sample 8	Sample 9
Download Pressure [psi]	0.4	0.7
Plate Speed [rpm]	50	70
Carrier Speed [rpm]	30	30
Time [min]	3	3

For this final round of polishing, a single three-minute polishing was used instead of three, one-minute polishings. This allows for an even greater comparability with Sample 1, the reference sample. The samples were cleaned immediately after polishing by undergoing a 10-minute ultrasonic bath submerged in IPA, followed by wiping down with an IPA soaked PVA sponge. Once wiped clean, the samples were dipped into IPA and dried with a nitrogen gun to prevent "water spots" from forming. Furthermore, since the etch rate across samples was somewhat inconsistent with all samples, exact regions before and after polishing/cleaning shall be compared using the profilometer.

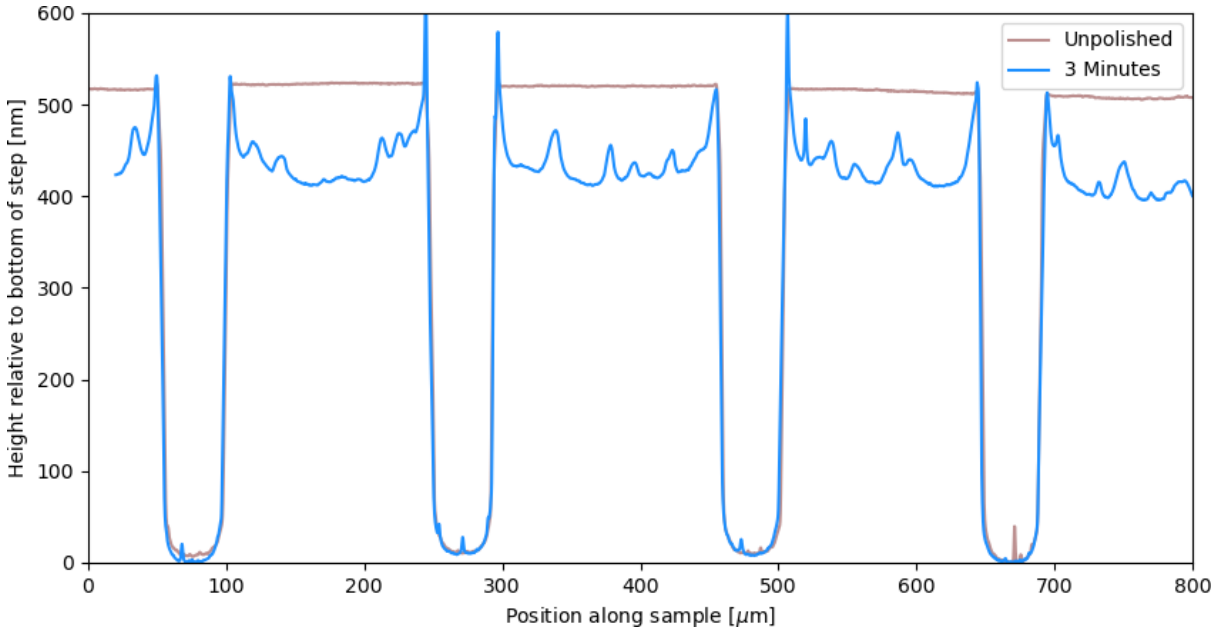

Figure 28: Profilometer data of Sample 8 before and after polishing/cleaning.

The profilometer data from Figure 28 clearly shows that etching has occurred on Sample 8, even though these same parameters (excluding cleaning and polishing frequency) had led to an apparent growth of the sample. Initially, this might make it seem as though the cleaning has removed a layer of particles, but the profilometer data appears to show remining particles on the surface. A look at optical microscope images of Sample 8 sheds light on both the now present etch rate, and the apparent remnant of particle contamination.

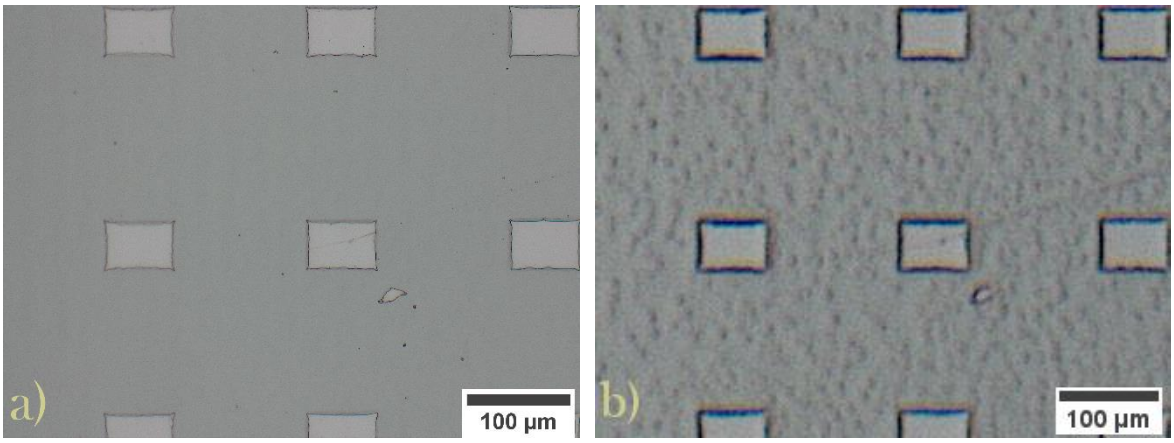

Figure 29: Optical microscope image of the region showed by the profilometer in Figure 28. a) shows the area seem through a 20X zoom lens, while b) is a digital zoom in of an image taken with a 2.5X lens

Figure 29 a, taken in the same region as the profilometer data in Figure 28, shows some small amounts of apparent particles on the surface, but nowhere near as much as the profilometer data would suggest. This leaves both the question of what is causing the surface roughness, and why there is now an etch occurring unanswered. Changing from the 20x optical zoom in Figure 29a, to the 2.5X optical zoom plus digital zoom in Figure 29b gives an answer to the apparent dirtiness of the sample. The surface now has a periodic surface roughness akin to that of an orange peel. This "orange peel" surface has been seen in other research [6] and appears to come from a too high concentration of citric acid.

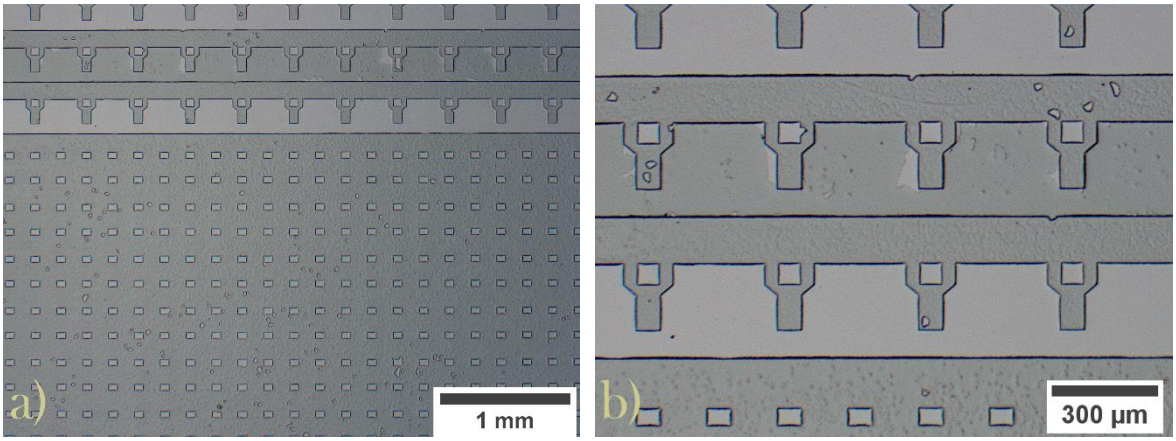

Figure 30:a) Optical microscopy image zoomed out from the region shown in Figure 29. b) a zoom in on the upper left of a) showing the "comb" feature.

Another clue to solving why Sample 3 had a growth rather than an etch appears at the top of Figure 30a (shown more clearly in Figure 30b), where one of the "combs" has become the same color as the bulk InSb surface. Normally, this region would be a brighter color, showing the presence of W on the bottom of the "comb". The fact that the color has now changed suggests that the W has been removed. To verify this, a further profilometer measurement, Figure 31, was conducted to run across a still light region of the grey "comb", over the gray portion of the same comb, and then across the entirety of a second "comb".

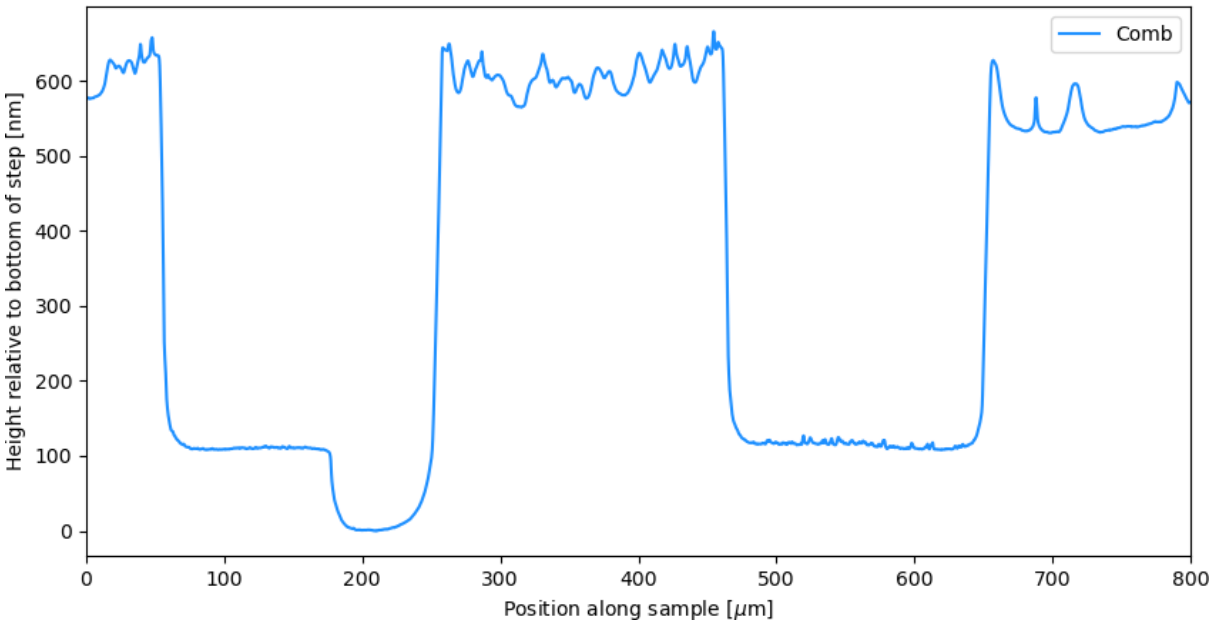

Figure 31: profilometer data running across two of the combs of Sample 8. The lowest dip corresponds to a gray portion of a comb.

Here in Figure 31, a clear dip can be seen below the surface of the tungsten at around 100 nm. This suggests that some of the tungsten has been removed by this polishing process. Interestingly, the difference between the bottom of the cleared portion and the tungsten surface is 100 nm, even though only 40 nm of tungsten was deposited. Since the polishing should only occur at the surface, it would appear that some wet etching occurs during this CMP process just from contact with the slurry. This should mean that lower etching times may be best for avoiding this added uncertainty. Notably, Sample 3 in Figure 19 exhibits this same

monochrome finish, though on a much larger scale. It is safe to say at this point that the growth that Sample 3 experiences was actually a lowering of the floor region through the removal of tungsten.

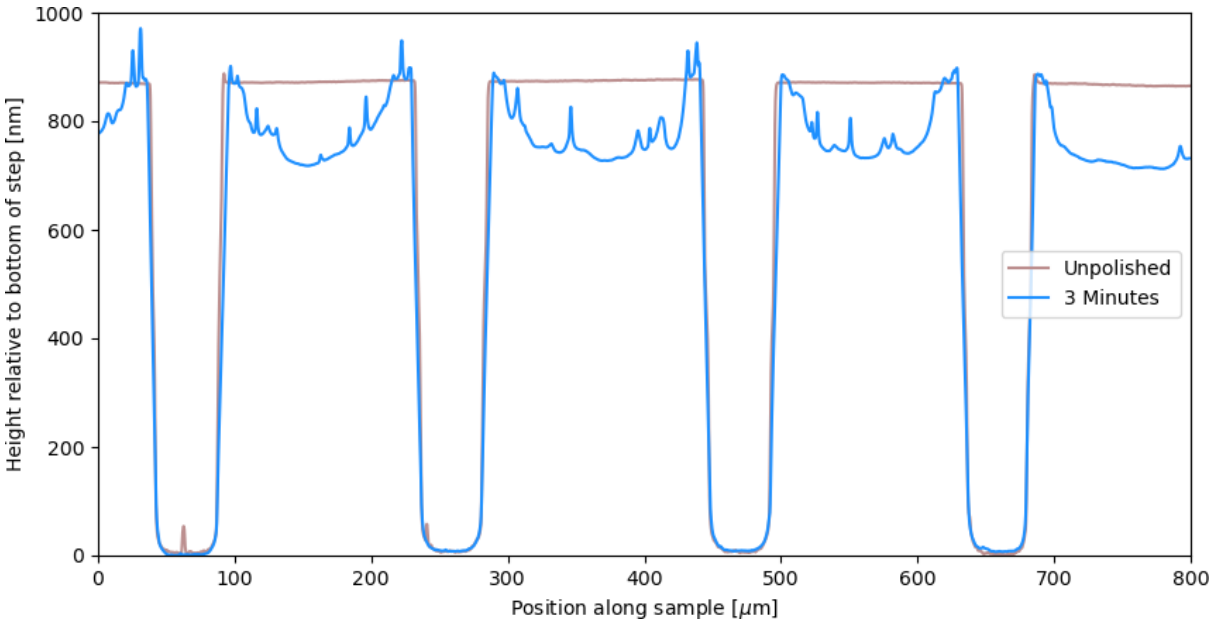

Figure 32: Profilometer data of Sample 9 before and after polishijng/cleaning.

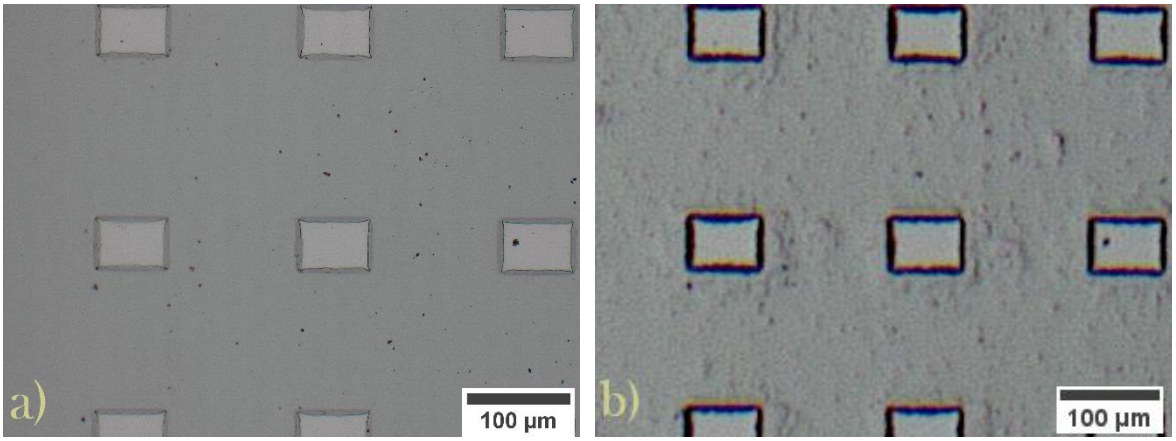

Figure 33: The surface of Sample 9 in the region where Figure 32 was taken. a) shows the area seem through a 20X zoom lens, while b) is a digital zoom in of an image taken with a 2.5X lens

Figure 33 shows that Sample 9 has more particles than Sample 8 did, though it is far cleaner than its sister sample, Sample 7, shown in Figure 23. Sample 9 shows the same "orange peel" surface that Sample 8 had, though to a lesser degree.

So far, from these two samples it can be said that the slurry used needs to contain less citric acid, that the slurry will wet etch the sample to some degree, that a certain download pressure needs to be met so as not to cleave tungsten from the surface, that having tungsten coated floors is an effective limit to floor wet etching, and that the cleaning method is of great utility, even if not quite perfect. Whether these samples remain clean on a nanoscale must be studied with AFM, as show in subplots b) and c) of Figure 34. It can be seen that the two samples have a cleanliness comparable to that of Sample 1, the other sample polished for 3 minutes in a row. The cleanliness does not noticeably exceed that of Sample 1, however, even though Sample 1

was cleaned with neither the ultrasonic bath nor the PVA sponge. While it is possible that these two samples would have been far dirtier on the nanoscale had they not been cleaned, they also remain comparable to their 3x1 counterparts. The one notable exception to this is that Sample 8 didn't have any hyper-dirty regions, like Sample 3 did, but this is perhaps more likely to do with less tungsten upheaval than better cleaning.

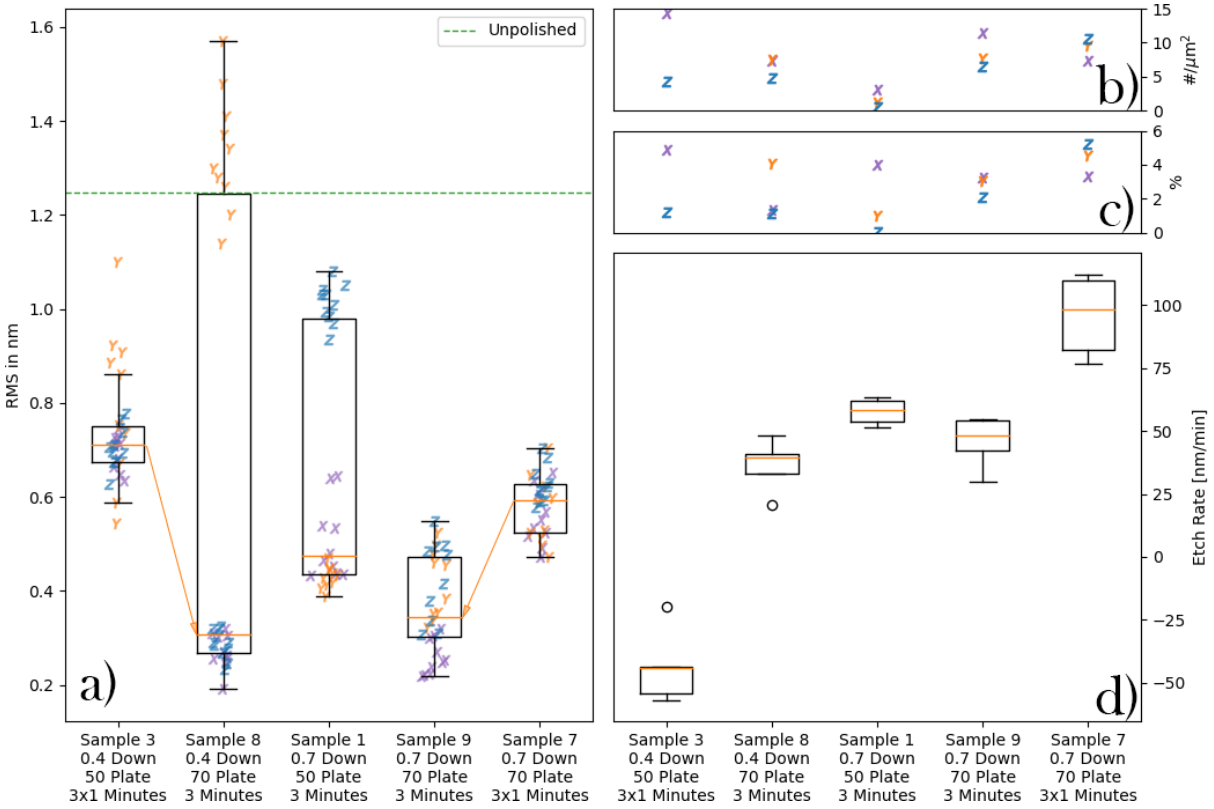

Figure 34: Various observed qualities for the samples polished for 3 minutes at once, along with the comparable parameters which were uncleaned and polished for three runs of 1 minute. a) shows the roughness distribution, b) the particle density at a nano scale, c) the relative coverage of these particles, and d) the etch rate for the parameters studied.

The etch rate for both samples can be seen compared to Samples 1, 3, and 7 in subplot d) of Figure 34. The etch rate for Sample 8 (with the minimum download pressure of 0.4 PSI) is now such that the sample gets smaller, rather than larger, in line with the other samples. At this point, it can be said with confidence that the growth which Sample 3 appeared to undergo was due to the removal of tungsten, rather than from the deposit of any new material. Oddly, the etch rate of Sample 9 is now considerably lower than that of Sample 7, which had one of the largest etch rates of the initial seven samples. One might expect that the samples which were uncleaned between polishing runs might experience greater etching from the particles on the samples acting as a sort of abrasive, but the etch data shown in Figure 10 does not show an accelerating etch rate, were the samples polish more and more with each successive run. Therefore, the most likely explanation is that the polishing pad (which is used for all CMP work, regardless of user) has worn down over time. The time in between polishing Sample 9 and Sample 7 was on the order of months, and so pad wear from other users polishings is a real possibility.

Finally, the surface roughness data shown in subplot a) of Figure 34 shows a comparable roughness between sister samples 9 and 7. There has been a slight reduction in roughness in Sample 9, indicating that single runs are more effective, but it could just as well be due to some

random uncertainty. Sample 8, however, makes a clear departure from Sample 3. In the X and Z regions, Sample 8 is far smoother, and is evenly matched with Sample 9. In the Y region, however, the sample is both rougher than an unpolished sample, but also has a broad spread in the value present.

A visual of Samples 8 and 9 on the nanoscale can be seen in Figure 35.

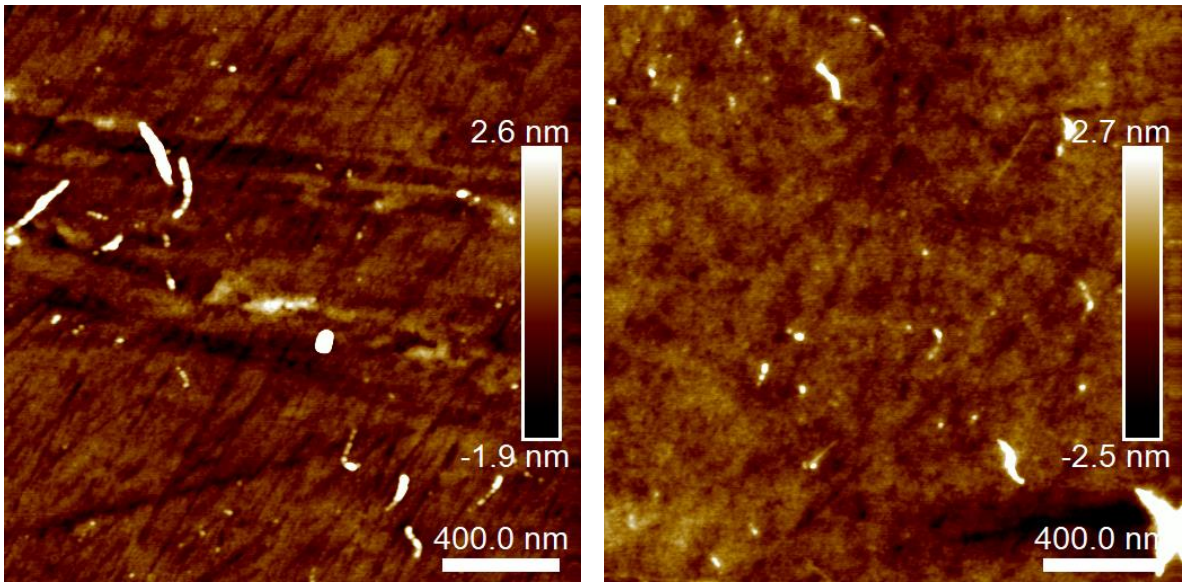

Figure 35: a) Sample 8 in region X. b) Sample 9 in region X.

Both samples are comparably clean in this region, and interestingly both have particles with heights of about 2.5 nm. This is in contrast to Figure 14 (which shows Sample 3) and Figure 13 (which shows Sample 7), who have particles of heights closer to 50 nm. Whether this difference is due to the cleaning performed or due to the single, longer runs used, it remains that the samples, while comparably dirty in terms of number and area are cleaner now in Samples 8 and 9 when considering volume. Also of note are the very apparent scratches on the surface of Sample 8. Sample 9 shows only a hint of scratching. These scratches, the sizable inconsistency in surface roughness's, and the ability to cleave W from the InSb surface makes the very low download pressures used in Samples 3 and 8 hard to recommend, except in the most specialized of circumstances.

5 Conclusion

Through this study it was found that InSb can be effectively polished using the CMP technique with a slurry of $NaOCl: DI(1{:}10) + C_6H_8O_7: DI(1{:}2)$. This slurry, however, results in a rough, textured surface, and so the slurry should be fine-tuned, most likely by reducing the concentration of citric acid used. This should also reduce the wet etch that happens during CMP, allowing for a more consistent etch rate which may be slow enough for nanometer precision. It was also found that to achieve a globally consistent etch rate, a higher downward pressure between the sample and polishing pad (such as in Sample 5) should be used. This comes with a tradeoff of a somewhat faster etch rate and inconsistently smooth surface on the nanoscale, suggesting that a finishing step should be used after. Such a finishing step could come from using a greater rotational plate speed (such as for Samples 7 and 9), as this had the tendency of making for a consistently smooth surface on the nanoscale. It was discovered that sample cleanliness is greatest in samples which are polished in one run (as in Samples 1, 8 and

9), and so these etch and finishing steps should occur in the same recipe. If a sample becomes dirty during the CMP process, ultrasonic baths are effective at dislodging larger particles, while PVA sponges can be used to remove smaller particles. These two cleaning methods, therefore, complement each other well. This cleaning is particularly effective on a global scale, though there may be some improvement on nanoscale debris as well. Usage of the PVA sponge should be gentle to avoid scratching, and an automated setup to provide a constant wiping pressure and speed would be of great utility.

Low download pressures (like for Samples 3 and 8) should be avoided when working with InSb and sputtered W. W very easily cleaves from the surface when the download is too low, and the resulting quality of InSb (in terms of surface roughness, cleanliness, and scratching) is too inconsistent to be relied upon. The one plus side to a low download is a slow etch rate. If the thickness of an InSb layer is more important than its smoothness, and if a short finishing step with a higher download and large plate speed is feasible, a low download could find use as part of a larger recipe.

6 Outlook

To improve upon these results, a selection of slurries could be used to polish several samples using a standard set of parameters. This could help to reduce the orange peel effect and to slow down the etch rate caused by wet etching. In the same line of thinking, the flow rate of the slurries could also be examined, to determine what affect, if any, this would have. The influence of pad age could be studied as well, by making baseline polishes of InSb samples over the course of a polishing pads lifetime. This would help to determine if a separate pad for softer III-V materials would be worth using. A cleaning method for CMP that is commonly used in the literature is megasonic bath cleaning [18], which employs frequencies in the range of 1-2 MHz which is more effective to remove small particles than ultrasound and could possibly better complement the PVA sponge. A megasonic bath was unfortunately not available for this project, but it would be worth installing such a tool in conjunction with the CMP lab.

Through this work, the bulk of the sample has been InSb, but there have been holes etched into it. This was vital for determining etch rate, but it is possible that the holes distribution, size, and density could have played a role in where and how etching occurred [19]. It could be studied how different masks influence the etch rate of InSb. It would also be of great interest to see how InSb deposited over other structures might polish. This could come in the form of InSb deposited over a surface with some raised features, or some lowered features. Both of these are closer to an actual industry application and would probably have significant implications for the etch rate of InSb in CMP.

Acknowledgments

To close out, I'd like to thank the people who have helped me to make this thesis a reality. Firstly, I want to thank my supervisor Mattias Borg for guidance and direction throughout this project. I imagine I would have had a tough time focusing myself to the task without him. Secondly, I'd like to thank everyone who helped me learn the ins and outs of all the various tools I needed to use in Lund Nano Lab. I can proudly say that with their training I managed not to break any multimillion kronor equipment. Thirdly I've got to thank my long bike rides, during which I always seemed to fit one more piece of the puzzle together. Finally, I'm lucky to have my amazing girlfriend Klara. She didn't give much science help, but that's not always what I needed.

References

[1] C. W. Kaanta, S. G. Bombardier, W. J. Cote, W. R. Hill, G. Kerszykowski, H. S. Landis, D. J. Poindexter, C. W. Pollard, G. H. Ross, J. G. Ryan, S. Wolff and J. E. Cronin, "Dual Damascene: a ULSI wiring technology," in *1991 Proceedings Eighth International IEEE VLSI Multilevel Interconnection Conference*, Santa Clara, CA, USA, 1991.

[2] J. H. Davies, The physics of low-dimensional semiconductors: an introduction, Cambridge, U.K. ; New York, NY, USA: Cambridge University Press, 1998.

[3] P. Mohan, S. M. Babu, P. Santhanaraghavan and P. Ramasamy, "Growth, phase analysis and mechanical properties of InSb1−xBix crystals," *Materials Chemistry and Physics*, vol. 66, p. 17–21, 9 2000.

[4] M. E. Levinshtein, S. Rumyantsev and M. Shur, Handbook series on semiconductor parameters, Singapore New Jersey London [etc.]: World scientific, 1996.

[5] H. Menon, N. P. Morgan, C. Hetherington, R. Athle, M. Steer, I. Thayne, A. Fontcuberta i Morral and M. Borg, "Fabrication of Single-Crystalline InSb-on-Insulator by Rapid Melt Growth," *physica status solidi (a)*, p. 2100467, 11 2021.

[6] S. Hayashi, M. Joshi and M. Goorsky, "Chemical Mechanical Polishing of Exfoliated III-V Layers," *ECS Transactions*, vol. 16, p. 295–302, 12 2019.

[7] "Tungsten Metal (W) Element Chemical + Physical Properties," 2 2014. [Online]. Available: https://www.tungsten.com/materials/tungsten/.

[8] "Wet Chemical Etching of Metals and Semiconductors," [Online]. Available: https://cleanroom.byu.edu/wet_etch.

[9] D. Zhao and X. Lu, "Chemical mechanical polishing: Theory and experiment," *Friction*, vol. 1, p. 306–326, 12 2013.

[10] J. M. Steigerwald, S. P. Murarka, R. J. Gutmann and D. J. Duquette, "Chemical processes in the chemical mechanical polishing of copper," *Materials Chemistry and Physics*, vol. 41, p. 217–228, 8 1995.

[11] H. Lee, B. Park and H. Jeong, "Influence of slurry components on uniformity in copper chemical mechanical planarization," *Microelectronic Engineering*, vol. 85, p. 689–696, 4 2008.

[12] P. B. Zantye, A. Kumar and A. K. Sikder, "Chemical mechanical planarization for microelectronics applications," *Materials Science and Engineering: R: Reports*, vol. 45, p. 89–220, 10 2004.

[13] K. Park, J. Oh and H. Jeong, "Pad Characterization and Experimental Analysis of Pad Wear Effect on Material Removal Uniformity in Chemical Mechanical Polishing," *Japanese Journal of Applied Physics*, vol. 47, p. 7812–7817, 10 2008.

[14] B. S. Kim, M. H. Tucker, J. D. Kelchner and S. P. Beaudoin, "Study on the Mechanical Properties of CMP Pads," *IEEE Transactions on Semiconductor Manufacturing,* vol. 21, p. 454–463, 8 2008.

[15] D. G. Thakurta, C. L. Borst, D. W. Schwendeman, R. J. Gutmann and W. N. Gill, "Pad porosity, compressibility and slurry delivery effects in chemical-mechanical planarization: modeling and experiments," *Thin Solid Films,* vol. 366, p. 181–190, 5 2000.

[16] C. J. Chen, "Atomic Force Microscopy," in *Introduction to Scanning Tunneling Microscopy,* Oxford University Press, 2021, p. 379–400.

[17] K. M. Krishnan, "Scanning Probe Microscopy," in *Principles of Materials Characterization and Metrology*, Oxford University Press, 2021, p. 745–802.

[18] I.-C. Choi, H.-T. Kim, N. P. Yerriboina, J.-H. Lee, L. Teugels, T.-G. Kim and J.-G. Park, "Post-CMP Cleaning of InGaAs Surface for the Removal of Nanoparticle Contaminants for Sub-10nm Device Applications," *ECS Journal of Solid State Science and Technology,* vol. 8, p. P3028–P3034, 2019.

[19] L. Wu and C. Yan, "An Analytical Model for Step Height Reduction in CMP with Different Pattern Densities," *Journal of The Electrochemical Society,* vol. 154, p. H596, 2007.